

NAB 2-153

DAA/AMES
Univ. of
California, San
Diego

48 pages

A Simulation Study of Two Major Events in the Heliosphere
During the Present Sunspot Cycle

S.-I. Akasofu¹, W. Fillius², Wei Sun^{1,3}, C. Fry¹ and M. Dryer⁴

¹Geophysical Institute
and

Department of Space Physics and Atmospheric Sciences
University of Alaska-Fairbanks
Fairbanks, Alaska 99701

²University of California, San Diego
La Jolla, California 92093

³On leave from
Institute of Geophysics
Academia Sinica
Beijing, China

⁴Space Environment Laboratory, NOAA
Boulder, Colorado 80303

Abstract

The two major disturbances in the heliosphere during the present sunspot cycle, the event of June - August, 1982 and the event of April - June, 1978, are simulated by the method developed by Hakamada and Akasofu (1982). Specifically, we attempt to simulate effects of six major flares from three active regions in June and July, 1982 and April and May, 1978. A comparison of the results with the solar wind observations at Pioneer 12 (~ 0.8 au), ISEE-3 (~ 1 au), Pioneer 11 (~ 7-13 au) and Pioneer 10 (~ 16-28 au) suggests that some major flares occurred behind the disk of the sun during the two periods. Our method provides qualitatively some information as to how such a series of intense solar flares can greatly disturb both the inner and outer heliospheres. A long lasting effect on cosmic rays is discussed in conjunction with the disturbed heliosphere.

(NASA-CR-176943) A SIMULATION STUDY OF TWO
MAJOR EVENTS IN THE HELIOSPHERE DURING THE
PRESENT SUNSPOT CYCLE (Alaska Univ.,
Fairbanks.) 48 p

N86-29756

CSSL 03B

Unclas

G3/92 43356

1. Introduction

The months of June and July, 1982 and of April and May, 1978 were two of the most active periods of the sun during the present solar cycle. There were at least three active regions during the first period and one region which produced a large number of flares, causing major disturbances in the heliosphere. For the first event, several shock waves and/or cosmic ray decreases were observed by deep space probes, Pioneer 12 (Venus orbiter) at about 0.7 au, Pioneer 11 at about 12 au and Pioneer 10 at about 28 au, as well as by the ISEE-3 at the libration point. A large decrease of cosmic ray intensity was observed at Pioneer 11 and 10 during this period (Fillius and Axford, 1984). Several major magnetic storms and two large Forbush decreases were also recorded at the earth during the same period. For the second event, a significant disturbance in the outer heliosphere was observed by Pioneer 11 at about 7 au and Pioneer 10 at about 16 au, manifested in the propagating shock waves and a large cosmic ray decrease, as well as two major geomagnetic disturbances, beginning on April 10 and 30, respectively. (Van Allen, 1979; McDonald et al., 1981; Intriligator and Miller, 1982; Burlaga et al., 1984).

The purpose of this paper is to attempt to simulate qualitatively the disturbances in the heliosphere during these two active periods using the method developed by Hakamada and Akasofu (1982), providing a first order construction, temporally and spatially, of flare-generated shocks and their multiple interactions with each other, as well as with corotating interaction regions. Other dynamic, thermodynamic, and magnetic properties (other than first-order IMF distortion) are not simulated and can only be found from the MHD solutions.

It is hoped that such a first order effort will be of some use in interpreting solar wind and cosmic ray observations by space probes. The

basis of this method is the distance (R) - time (t) relationship which can be obtained from the empirically constructed velocity (V) - distance (R) relationship from space probe observations. A theoretical V-R relationship (based on MHD solutions) can also be used to infer the R-t relationship. Olmsted and Akasofu (1984) demonstrated in detail the compatibility of our method with the MHD methods as far as the V-R and R-t relationships are concerned. Akasofu and Hakamada (1983) have already tested their method for successive six hypothetical flares from the same active region.

2. Event of June - August, 1982

Figure 1 shows the H α synoptic charts for Carrington Rotations 1722, 1723 and 1724 (Solar-Geophysical Data, no. 455, 456, 457 and 458). The three active regions are labeled as A, B and C. These regions were relatively short lived. Region A disintegrated after Carrington Rotation 1722, so that it is not seen in Carrington Rotation 1723. Region B was weakened during Carrington Rotation 1724. During Carrington Rotation 1724, Region C became the most active region. The H α filtergram profiles around the central meridian passage of the three regions A, B and C are shown in Figures 2a (June 8), 2b (June 21) and 2c (June 18), respectively. Table 1 lists some of the major flares produced by the three regions and the storm sudden commencements (ssc's) which were inferred to be associated with the flares.

Among the flares, we have chosen those which could, with reasonable confidence, be associated with an identifiable interplanetary shock wave at ISEE-3 and a ssc at the earth. The chosen flares are numbered, 1, 2, 3...7 as listed in Table 1; note that some of the flares are not numbered, because it was not possible to identify the resulting ssc for them; as we shall see later, it is not possible to simulate the associated event, since we cannot infer the flow speed from the transit time. However, the 'flares' no. 4a and

4b are not observed ones and will be discussed later. Figure 3 shows the location of the flare, Venus (Pioneer 12), Earth, Pioneer 10 and 11 at the time of the eight flares. In this paper, our heliographic longitude is fixed in a heliospheric inertial frame. This frame is aligned with the commonly used heliocentric equatorial system, HEQ. In the HEQ system, the z axis is parallel to the solar rotational axis, x is directed along the intersection of the equatorial and ecliptic planes. This intersection is about 75° from the point Aries in the direction of the earth's orbital motion. More precisely HEQ x-axis is rotated by $74^\circ 22' + 84' T$, where T is the centuries since 1900. The y-axis is formed by the right hand rule. Our heliographic longitude = 0° line (the x-axis) is rotated by an angle α with respect to the HEQ x-axis. We choose our heliographic longitude to coincide with Carrington longitude at the simulation start time, $T_F = 0$. Of course, as the simulation time progresses, the sun rotates and carries the Carrington coordinate system along, while our heliographic coordinates are fixed in space. As a point of reference, for the 1978 simulation, our heliographic longitude = 0° line lies at HEQ longitude = 101° , or heliocentric ecliptic, HEC, longitude = 176° , HEC latitude = 7.1° . In the 1982 simulation our 0° line lies at HEQ longitude = 162° , and HEC longitude = 238° , HEC latitude = 2.2° .

A wide longitude and distance coverage of monitoring disturbances in the heliosphere make this particular period unique. Figure 4 shows, from the top, the solar wind speed observed at Pioneer 10, 11 and 12 (A. Barnes, private communication) and the magnetic field magnitude observed at ISEE-3 (E. J. Smith, private communication). One of the most remarkable features in Figure 4 is the two shock waves observed at Pioneer 10 on July 30 and at Pioneer 11 on August 3, respectively. Figure 5 shows the energetic particle data at Pioneer 10 and 11 and the neutron monitor record at Deep River for the period

between 1980 and 1983 (Fillius and Axford, 1984). Note in particular decreases of the energetic particle fluxes at Pioneer 10 and Pioneer 11 in July and August, 1982 and the two large Forbush decreases at the earth in July. Recent new observations by deep space probes have also revealed that shock waves generated by successive solar activities advance well into the outer heliosphere and cause considerable disturbances of the solar wind and of the interplanetary magnetic field structure, resulting in reduction of the intensity of galactic cosmic rays (Van Allen, 1976; McDonald et al., 1981; Smith, 1982; Burlaga, 1982; Burlaga et al. 1984). This figure will be discussed in detail after describing our simulation results.

It is of great interest to follow how the shock waves generated by the flare activity disturbed the heliosphere at two widely separated points, as well as at the earth. During the last several years, considerable progress has been made in understanding the propagation of solar wind disturbances in the heliosphere. The exploration of the outer heliosphere by deep space probes has recently added much new information on the general conditions of the solar wind and the magnetic field. In particular, the propagation of solar wind disturbances in the heliosphere has recently been studied extensively, both theoretically and observationally (cf. Dryer, 1974, 1975, 1984; Dryer and Steinolfson, 1976; Smith et al., 1977; Wu et al., 1977, 1983; Dryer et al., 1976, 1984; Intriligator, 1977; Smith and Wolfe, 1979; Wu, 1980; Wu et al., 1977, 1979, 1983; Han et al., 1984; Gislason et al., 1984).

The theoretical studies of the propagation of flare-generated shock waves are based on hydrodynamic or MHD methods which require considerable computation. To simulate such complicated features in the outer heliosphere requires simultaneous solution of the MHD equations by finite-differencing techniques. At the present time, however, it is difficult to simulate by the MHD method an

extensive event associated with a large number of successive flares, superimposed on the corotating interplanetary regions (CIR). It is for this reason that Hakamada and Akasofu (1982) devised a simple 'kinematic' method in simulating some aspects of the disturbed solar wind.

During the course of our study, we have found that it is difficult to explain some of the major outer heliosphere events at Pioneer 12 on July 2 and at Pioneer 10 on July 30 only on the basis of the observed six flares, as well as of some less intense flares which were not listed in Table 1. We infer thus that there must have been intense flares behind the solar disk at Region A on about June 20 and at Region B on about July 1. There is no reason why active regions have to produce flares only when they are facing toward the earth. Further, there was no other major active region to cause heliospheric disturbances in the direction of Pioneer 12 and Pioneer 10 during this particular period. By including such hypothetical flares (no. 4a and 4b in Table 2), we attempt to explain the solar wind observations at Pioneers 10, and 12 and IMF observations at ISEE-3.

a. Basic Flow Pattern

We simulate first the basic flow pattern into which the disturbances generated by the seven flares are introduced. It is assumed that the heliomagnetic equator determined by Hoeksema et al. (1983) for the Carrington rotation 1722 (May 19-June 14) can be approximated by a two-stream (or so-called 'two-sector') situation and that the heliomagnetic equator remained the same during the Carrington rotations 1723 and 1724 (June 15-July 11 and July 12-August 8); this is a reasonable assumption on the basis of inspection of the heliomagnetic equator for the rotations 1722, 1723 and 1724, determined by Hoeksema et al. (1983). In our simulation procedure, this situation is equivalent to assuming that the solar "dipole axis" is inclined with respect

to the rotation axis by angle χ which is taken to be 20° in this particular period or that the heliomagnetic equator is given as $\chi \sin(\phi + \phi_0)$ with respect to the heliographic equator where ϕ and ϕ_0 denote the longitude and phase angle, respectively. The solar wind speed V is assumed by Hakamada and Akasofu (1982) to increase towards higher magnetic latitude θ as follows:

$$V \text{ (km/sec)} = 700 \left(1 - \frac{1}{\cosh(0.06 |\theta|)}\right) + 300 \quad \text{for } 0 < |\theta| < 30^\circ$$

$$V \text{ (km/sec)} = 775 \quad \text{for } 30^\circ < |\theta|$$

The upper panel in Figure 6a shows the solar wind speed distribution on the source surface (of a spherical shell of 2.5 solar radii). In this way, the earth (located at latitudes $\theta \leq 7^\circ$) encounters a flow from the northern latitude during one-half of Carrington Rotation and a flow from the southern hemisphere during the other half. The flow pattern thus generated produces the familiar spiral interplanetary magnetic field (IMF) pattern with the alternating (toward and away) polarity, together with the two 'spiral arms', namely the CIRs.

In this paper, we shall see how such a basic IMF pattern was disturbed by a series of solar flare-generated shock waves which took place in June and July 1982. We construct also the velocity (V) - time (t) pattern at Pioneer 10, 11 and 12 and compare it with the observations. For details of the procedure of establishing the basic flow pattern, see Hakamada and Akasofu (1982). For the rest of the panel of Figure 6, see (b).

b. Solar Wind Disturbances Induced by Flares 1, 2, 3, 5, 6 and 7

In our simulation procedure, each flare is characterized by seven parameters; they are the onset time T_F , heliographic longitude ϕ , latitude θ , the maximum speed V_F generated by the flare, the time variations of V character-

ized by τ , the extent characterized by the half width of the Gaussian distribution σ° and the deceleration parameter α (Hakamada and Akasofu, 1982). As an example, the middle panel in Figure 6a shows the solar wind speed distribution generated by the flare no. 1, which is characterized by $\phi = 302.4^\circ$, $\theta = -12^\circ$, $V_F = 820$ km/sec, and $\sigma = 80^\circ$ at the maximum epoch. The time variations of the maximum speed for the first flare ($\tau = 5$ hrs.) are shown at the bottom panel of Figure 6a; note that the speed reaches the maximum value (820 km/sec) five hours after flare onset.

Table 2 gives the seven parameters chosen for our flares 1, 2, 3, 5, 6 and 7, as well as for the hypothetical flares 4a and 4b (which will be discussed in section c). The time for our simulation study is reckoned from 1900 UT, May 18, the zero-th day of Carrington Rotation 1722. For each flare, the onset time T_F , the longitude ϕ and latitude θ can directly be determined from the observations. The speed V_F , the deceleration parameter α , as well as τ and σ , must be determined on a trial and error basis in such a way that the arrival time of each shock wave at the earth and Pioneer 10 and 11 agrees approximately with the observations. Obviously, the choice of the parameters is not unique. In our method, there is no way, at the present time, to determine V_F , τ , σ and α (or any other combinations of different sets of parameters which characterize a flare) uniquely. Any modeling effort of this kind would suffer from a similar non-unique problem with different degrees. One of the difficulties associated with this problem can be realized by noting that many flares occur far from the central meridian and thus that only the skirt of the shock wave reaches the earth. The shock speed may depend greatly on the angle between the solar center-flare line and the direction of propagation, and this dependence may be different for different flares. Figure 6b shows the total (quiet plus flare-generated) solar wind speed distribution at the maximum

epoch of each of the eight flares including that for flares no. 4a and 4b.

Figures 7a-f show the solar wind disturbances caused in the inner heliosphere (< 2 au) by the flares 1, 2, 3, 5, 6 and 7 at the time of the arrival of the shock wave (at the time of the ssc for each flare) at the earth which is indicated by the mark*. None of the six flares occurred near the central meridian of the solar disk, so that only the skirt of the shock passed by the earth. The shock waves must often extend well beyond $\pm 45^\circ$ in longitude from the flare longitude in order to explain the arrival at the earth (cf. Akasofu and Yoshida, 1967; Chao and Lepping, 1974; Dryer, 1974).

Figures 8a and 8b show the disturbed solar wind in the outer heliosphere by the six flares; 1, 2, 3, 5, 6 and 7 at $T = 1752$ hr (73.0 day, July 30) and $T = 1848$ hr (77.0 day, August 3), respectively (Figure 4). The location of Pioneer 10 (~ 28 au) and Pioneer 11 (~ 12 au) are indicated by the * mark. These dates correspond to the dates of the observation of the shock wave at Pioneer 10 and Pioneer 11, respectively; see Figure 4. One can see the passage of a 'coalesced' shock at the location of Pioneer 11 at $T = 1848$ hr (77.0 day, August 3). However, it is not possible to explain the Pioneer 10 observation at $T = 1752$ hr (73.0 day, July 30) on the basis of the observed six flares, 1, 2, 3, 5, 6 and 7. Region C caused a few other flares after July 14 in the western hemisphere of the solar disk. In order for them to be responsible for the solar wind and energetic particle observations at Pioneer 10, unreasonably high speed flows are required, since the shock waves would have traveled about 28 au in less than 20 days.

c. 'Flares 4a and 4b'

One of the possibilities to overcome this difficulty is to assume that there occurred two intense flares behind the visible disk of the sun on about June 20 and July 1, respectively. One of the reasons for suspecting it was

that the first active region A went behind the western limb on June 14, and the second active region B went behind the western limb of the sun on June 27. From Figure 1, it is difficult to find any other active regions as the source(s) in explaining the intense shock waves observed at Pioneer 12 and Pioneer 10. Both Regions A and B were quite active near the western limb.

The simulation study is complicated by the fact that no major increase of the solar wind was observed on June 21 or 22 at Pioneer 12 which was located only 40° in longitude from Pioneer 10. It appears thus that the shock wave from Region A must have occurred on or before June 20 and must have been narrowly confined in longitude. We assume that a hypothetical flare designed as flare no. 4a occurred on June 16, although such an assumption is a very tentative one.

There was also a large increase of the solar wind speed at Pioneer 12, from 469 km/sec on July 1 to 628 km/sec on July 2. Since the only active region facing Pioneer 12 was Region B, we infer that there occurred a fairly intense flare on July 1, which we designate as flare no. 4b. Another supporting evidence of this hypothetical flare is the IMF disturbances observed by ISEE-3 on July 5-6 (see Figure 4). There were no significant solar activity between July 1 and July 5, so that it is possible that this particular disturbance was caused by the hypothetical flare no. 4b; the skirt of the simulated shock wave must have passed by the earth on July 5. This situation is illustrated in Figure 9a and 9b in which the location of the shock wave at $T = 1133$ hr (47.2 day, July 5) is shown. Unfortunately, it is not possible to associate this particular flare as the cause of the event at Pioneer 10 on July 30, since an exceedingly high speed flow and the resulting shock wave are required.

Figures 10 show the heliospheric disturbances in the ecliptic plane at $T = 1437$ hr (59.9 day, July 17), 1651 hr (68.8 day, July 26), 1752 hr (73.0 day,

July 30) and 1848 hr (77.0 day, August 3) by including the hypothetical flares 4a and 4b. Thus, what appears to be a single major heliospheric event in Figures 4 and 5 may result from a number of flares, including some behind the disk. We attempt to substantiate this claim a little more quantitatively in (d).

d. The Velocity (V) - time (t) Relationship

Figure 11 shows the V-t relationship at the location of Pioneer 10, 11 and 12, respectively as well as at the location of the earth. They may be compared with the corresponding data in Figure 4. The V-t curves at Pioneer 10, 11 and 12 have fair resemblance to the observed ones, as far as the two shock waves are concerned. However, much of the corotating structures seem to degenerate at the location of Pioneer 10 (28 au), since they are not very evident in Figure 4. On the other hand, some of them can be seen clearly at the location of Pioneer 11 (13 au). It may be that many fine structures at Pioneer 12 are difficult to explain without including less intense solar activities. Note that it is also possible to identify tentatively some of the peaks observed at ISEE-3 with the computed peaks.

3. Event of April - June, 1978

Region 15266 of the sun caused a profound disturbance in the outer heliosphere, and this subject has already been the source of several papers during the last several years. In particular, a flare of importance 3B at 1304 UT on April 28, 1978 was considered to be responsible for the intense shock wave and the large decrease of cosmic-ray intensity observed at Pioneer 11 at ~7 au on May 11 and Pioneer 10 at ~16 au on June 5 (Pyle et al., 1979; Van Allen, 1979; McDonald et al., 1981; Intriligator and Miller, 1982; Burlaga et al., 1984). Other intense shock waves were observed at Pioneer 10 on May 27 and at Pioneer 11 on May 8. Actually, region 15266 had been quite active at least from the

day when it appeared near the eastern limb and caused a number of flares during the period when it was facing the earth (Dodson and Hedeman, 1981). There was at least another active region, region 15221, which caused several flares during the first week of April.

Therefore, in order to study the major heliospheric disturbances in April and June 1978, it is important to examine how the shock wave generated by each flare propagated in the heliosphere and then how all the shock waves contributed to the overall disturbances. Indeed, the intense Forbush decrease which began on April 30 showed a three-stage decrease; the main phase of the geomagnetic storm which began on April 30 had deepened until May 4. Both phenomena indicate that effects of the successive flares accumulated.

In this paper we have chosen six intense flares of importance greater than 2 in April and May, 1978 and tentatively identified the corresponding ssc's; they are also listed in Table 3. Such identifiable ssc's are likely to be an important evidence for the generation of interplanetary shock waves.

Pyle et al. (1979) noted that the shock waves observed at Pioneer 10 on May 27 and at Pioneer 11 on May 8 cannot be explained without invoking an intense flare on the backside of the solar disk on about April 15. Intriligator and Miller (1982) inferred that this particular flare occurred in region 15266. There was no highly active region within $\pm 90^\circ$ centered around region 15266, so that this choice seems to be reasonable. However, this particular region was at about 75° in heliographic (or Carrington) longitude, while the earth was at about 285° , so that in their Figure 1, λ should be 27° , instead of 60° . This particular flare is designated as flare no. 3 in Table 3. However, although it is very tentative, it is our finding that the space probe observations appear to be explained better by supposing that the responsible flare occurred on April 17, instead of April 15. After the completion of this

study, we have learned that the Voyager-1 and -2 spacecraft observed a very important kilometric radio Type II event by the Planetary Radioastronomy Experiment on April 17, 1978; both spacecraft were behind the solar disk at that time (Y. Leblanc, private communication, 1984). Figure 12 shows the location of seven flares and of Pioneers 10 and 11, as well as of the earth, at the time of each flare listed in Table 3.

The basic solar wind flow pattern in April - June, 1978, was different from that in June - August, 1982 in that the "four-sector" structure prevailed in the April - June, 1978 period (Hoeksema et al., 1983), while the "two-sector" structure did in the June - August, 1982 period. In our method, the "four-sector" structure is simulated by assuming that the heliospheric magnetic equator is given by $\chi \sin (2\phi + \phi_0)$, instead of $\chi \sin (\phi + \phi_0)$. Four high speed streams and four "spiral arms" result from such a situation, instead of two high speed streams and two "spiral arms" in the "two-sector" situation. In this paper, χ is taken to be 20° .

We introduce the seven flares into the "four-sector" situation thus determined. Table 4 gives the seven parameters for each flare. In this paper, the deceleration parameter α is taken to be 1000 for all the flares except for no. 4 flare ($\alpha = 2000$). The flare parameters must be determined on a trial and error basis, and in particular the April 28 flare (no. 4) had a very large σ value ($\approx 190^\circ$). Such a large value of σ is needed, if this particular flare was responsible for the shock wave observed at both Pioneer 11 on May 11 and Pioneer 10 on June 4.

Figure 13 shows the geometry of the six shock waves generated by flares nos. 1, 2, 4, 5, 6, and 7, respectively, and their relationship to the four-sector structure at the time when they reached the earth (causing ssc's). Since flare no. 3 occurred almost on opposite side of the earth with respect

to the sun, it is difficult to identify the associated ssc. Intriligator and Miller (1982) suggested that an ssc on April 17 was caused by the flare no. 3. However, such an identification should be considered only very tentative; there was some indication that weak recurrent geomagnetic storms occurred successively about 27 days apart during this period, beginning on January 18, and then February 25, March 22 and April 17.

One of the interesting features in Figure 13 is that the inner heliosphere was almost completely surrounded by the "coalesced" shock waves, namely the four spiral arms and the shock wave generated by flare no. 4 (April 28) and could be an important cause for the major Forbush decrease. Such a unique situation was caused partially by a large value of σ for flare no. 4 and could be an important cause for the major Forbush decrease.

Figure 14 shows "snapshots" of the propagating heliospheric disturbances on May 8, 11, 27 and June 5. Those are chosen on the basis of Table 1 in Intriligator and Miller (1982). It should be recalled that the shock waves were observed at Pioneers 10 on May 27 and June 5 and at Pioneer 11 on May 8 and 11. In this simulation study, it is assumed that there was no flare activity after May 1. As a result, the four-sector pattern began to develop in the inner heliosphere after May 1. Actually, there were two other intense flares (May 11 and May 31) which disturbed the inner heliosphere. Thus, the present simulation may serve in illustrating how a quiet condition might reappear after the end of an intense solar activity.

Figure 15 compares the observed velocity profiles at Pioneers 10 and 11 with the computed ones. The observed velocity profiles are taken from Intriligator and Miller (1982). The major features of the velocity variations are fairly well reproduced at both Pioneers 10 and 11, indicating that our simulation may be a fair representation of the actual conditions to a distance of

about 7-10 au. However, the shock wave generated by the April 28 flare appeared to degenerate considerably at the distance of Pioneer 10 (16 au). Thus, the shock structure which passed Pioneer 10 on June 5-13 could not be reproduced, although the decay part (after June 13) may have some resemblance.

4. Discussions and Conclusions

It is hoped that the simulation method adopted here is of some use in providing some idea about the geometry of the heliospheric disturbances in June - August, 1982 and April - June, 1978. It is possible that the heliosphere was much more disturbed by other unseen major flares and weaker flares which are not included in this study. For the June - August, 1982 event, the simulated velocity-time profile at both Pioneers 10 and 11 has a fair resemblance to the observed ones, suggesting that the major disturbances are simulated with fair accuracy. For the April - June, 1978 event, the fair agreement between the observed and simulated velocity variations at Pioneer 11 suggests that the simulated heliospheric disturbance patterns in the outer heliosphere to a distance of about 10 au are a fair first approximation; however, the shock appeared to degenerate considerably by the time it reached Pioneer 10 (16 au), so that our simulation results are likely to be much less accurate at distances greater than 15 au.

The two solar events produced a profound effect in the cosmic ray intensity observed at Pioneers 10 and 11, as well as at the earth (Figure 5). The cosmic ray variations during the April - June, 1978 event was described in detail by Van Allen (1979) and McDonald et al. (1981). Extending the impulse response function analysis by Bowe and Hutton (1982), Akasofu et al. (1984) have recently shown that a high (monthly) occurrence of major flares maintains some identity, in terms of its effect on cosmic-ray intensity, for as long as 17 months. One could envisage that the disturbed structure which has some

resemblance to what we have simulated in this paper is propagated outward in the outer heliosphere for more than one year. It appears that the accumulated effects of such solar activity may have an important contribution to the 11-year modulation in the cosmic-ray intensity. In fact, one of the motives for studying the June - August, 1982 episode is the effect which it had on galactic cosmic rays. During this short interval the cosmic ray intensity decreased by an amount equivalent to half the amplitude of the eleven year solar cycle (Fillius et al., 1983; Fillius and Axford, 1984). This feature is well illustrated in Figure 5. We see two declining epochs and two recovery epochs. The 1980 portion of this graph, up to the first cosmic ray minimum in early 1981, is part of a prolonged decline which began in 1978, from solar minimum conditions to solar maximum (Burlaga et al, 1984). The apparent recovery phase beginning in 1981 brought the intensities about halfway back to solar minimum values before being interrupted by the June - August, 1982 events. The decrease in this short interval took the cosmic ray intensities back down to minimum values. Finally we see the more enduring increase that has lasted to the present time. Solar particle events interrupted the Pioneer 11 curve in May, 1981, and again from June 6, 1982 until the decrease in early July.

The first decline appears to be the sum of many stepwise events of different magnitudes, which propagated outward at approximately the solar wind velocity, and frequently correlated with solar wind features (McDonald et al., 1981; McKibben, et al., 1982; Webber and Lockwood, 1981). However, the nature of these features remains elusive, with many suggestions such as bubbles, shocks, corotating interaction regions, and transient interaction regions (Newkirk et al., 1981; Perko and Fisk, 1983; Burlaga et al., 1984).

The second decline is the largest concentrated change in at least a de-

cade since the previous solar maximum in 1972. From the positions of the Pioneer spacecraft (Figure 3), we can see that the effect is large, not just in amplitude, but in spatial extent. The Pioneer spacecraft are on opposite sides of the sun, and the decrease evidently engulfed the entire heliosphere. It is evident that we need to look at solar wind structures on the same scale, and in three dimension, to visualize the processes affecting the cosmic rays. The kinematic method used in this paper is, at present, the only method available to model solar wind interaction regions on this scale. Whether or not these images are accurate in all detail, they do demonstrate that, when many flares occur during one or more solar rotations, they can produce interplanetary structures on a global scale. It is quite plausible that such global structures have an especially strong cosmic ray modulation effect.

Table 5 lists the times of occurrence of some of the features that are identifiable in the data (Figures 4 and 5) and in the model (Figures 8, 10 and 11). Of course, the model matches the solar wind data, by design, in as much detail as the modeling has been carried out. At certain times, there is a timing mismatch between solar wind and cosmic ray features that are certainly related (namely, the August events at Pioneer 11). This is not a modeling defect, because it is visible in the very data. It would be of interest to carry out a detailed study of the solar wind structures in high time resolution and to try to clarify, using magnetic field data, the relationship between the solar wind and cosmic ray features. However, such a study is beyond the scope of this paper.

Also, it is quite noticeable that, following the initial Pioneer 10 cosmic ray decrease of July 30 - August 3, there are two more step decreases approximately 25 and 50 days later. These echo decreases do not seem to correspond

to any features in the solar wind velocity at Pioneer 10 - another interesting puzzle. In the absence of local structures to produce the modulation, we should be forced to hypothesize non-local structures, for which there are certainly not enough data to constrain our models. Unfortunately, there are no data from the Pioneer 10 magnetometer to aid our understanding. The most likely explanation seems to be that the cosmic rays are modulated by magnetic field structures not evident in the solar wind velocity data.

Acknowledgements: The work reported here is supported in part by a grant from the National Aeronautics and Space Administration (NSG7447) and the National Science Foundation, Atmosphere Sciences Section (83-12515). We would like to thank Dr. E.J. Smith, JPL, and Dr. A. Barnes, NASA Ames Research Center, for providing us with the ISEE-3 and the Pioneer data which are used extensively in this paper. We thank also one of the referees and Dr. Y. Leblanc, Observatory of Paris, Meudon, for their information on the radio observation on April 17, 1978.

*The final proof will contain an
acknowledgement of NASA Grant NAS2-153*

References

- Akasofu, S.-I. and S. Yoshita, The structure of the solar plasma flow generated by solar flares, Planet. Space Sci., 15, 39, 1967.
- Akasofu, S.-I., C. Olmsted and J.A. Lockwood, Solar activity and modulation of the cosmic-ray intensity, J. Geophys. Res. (submitted, 1984).
- Akasofu, S.-I. and K. Hakamada, Solar wind disturbances in the outer heliosphere, caused by six successive solar flares from the same active region, Geophys. Res. Lett., 10, 577, 1983.
- Bowe, G.A. and C.J. Hatton, A study of the modulating effects of solar flares on the cosmic-ray intensity using time series analysis, Solar Phys., 80, 351, 1982.
- Burlaga, L.F., Interplanetary observations of driven shocks, EOS, 63, 1087, 1982.
- Burlaga, L.F., Understanding the heliosphere and its energetic particles, Invited Rapporteur Paper, Eighteenth International Cosmic Ray Conference, Vol. 12, 21, 1983.
- Burlaga, L.F., R. Schwenn and H. Rosenbauer, Dynamical evolution of interplanetary magnetic fields and lows between 0.3 au and 8.5 au: Entrainment, Geophys. Res. Lett., 10, 413, 1983.
- Burlaga, L.F., F.B. McDonald, N.F. Ness, R. Schwenn, A.J. Lazarus and F. Mariani, Interplanetary flow systems associated with cosmic-ray modulation, J. Geophys. Res. 89, 6579, 1984.
- Chao, J. and R.P. Lepping, A correlating study of sec's, interplanetary shocks, and the solar activity, J. Geophys. Res. 79, 1799, 1974.
- Dodson, H.W. and E.R. Hedeman, Experimental comprehensive solar flare indices for "major" and certain lesser flares, UAG-80, World Data Center A for Solar-Terrestrial Physics, NOAA, Boulder, Colorado, July, 1981.

Dryer, M., Interplanetary shock waves generated by solar flares, Space Sci. Rev., 15, 403, 1974.

Dryer, M., Interplanetary shock waves: Recent developments, Space Sci. Rev., 17, 277, 1975.

Dryer, M., Interplanetary evolution of solar flare-generated disturbances and their potential for producing magnetic activity, Proc. Internat. Workshop on Solar Physics and Interplanetary Travelling Phenomena, Kuming, China, Science Press, Beijing, 1984.

Dryer, M. and R.S. Steinolfson, MHD solution of interplanetary disturbances generated by simulated velocity perturbations, J. Geophys. Res., 81, 5413, 1976.

Dryer, M., Z.K. Smith, R.S. Steinolfson, J.D. Mihalov, J.H. Wolfe and J.K. Chao, Interplanetary disturbances caused by the August 1972 solar flares as observed by Pioneer 9, J. Geophys. Res., 81, 4651, 1976.

Dryer, M., S.T. Wu, G. Gislason, S.M. Han, Z.K. Smith, J.F. Wang, D.F. Smart and M.A. Shea, Magnetohydrodynamic modelling of interplanetary disturbances between the sun and the earth, Astrophys. Space Sci., 187, 1984.

Dryer, M., S.T. Wu and S.M. Han, Two-dimensional, time-dependent MHD simulation of the disturbed solar wind to representative flare-generated and coronal hole-generated disturbances, Geofiscia Internacional, 19, 1-5, 1980.

D'Uston, C., M. Dryer, S.M. Han and S.T. Wu, Spatial structure of flare-associated perturbations in the solar wind simulated by the two-dimensional numerical MHD model, J. Geophys. Res., 86, 525, 1981.

Fillius, W. and W.I. Axford, Large scale solar modulation of >500 MeV/N galactic cosmic rays seen from 1-30 au, J. Geophys. Res., (in press), 1984.

Gislason, G., M. Dryer, Z.K. Smith, S.T. Wu and S.M. Han, Interplanetary disturbances produced by a simulated solar flare and equatorially-fluctuating heliospheric current sheet, Astrophys. and Space Sci. 98, 149, 1984.

Hakamada, K. and S.-I. Akasofu, Simulation of three-dimensional solar wind disturbances and resulting geomagnetic storms, Space Sci. Rev., 31, 3, 1982.

Han, S.M., S. Panitchob, S.T. Wu and M. Dryer, A numerical simulation of three-dimensional transient ideal magnetohydrodynamic flows, presented at Southeastern Conference on Theoretical and Applied Mechanics, May 1984, Proceedings, Vol. II, pp. 39-45, Auburn University, AL.

Hoeksema, J.T., J.M. Wilcox and P.H. Scherrer, The structure of the heliospheric current sheet: 1978 - 1982, J. Geophys. Res., 88, 9910, 1983.

Intriligator, D.S., Pioneer 9 and Pioneer 10 observations of the solar wind associated with the August 1972 events, J. Geophys. Res., 82, 603, 1977.

Intriligator, D.S. and W.D. Miller, Plasma shocks and energetic particles in the outer solar system: Trapping and asymmetry observations from Pioneer 10 and Pioneer 11, J. Geophys. Res., 87, 4354, 1982.

McDonald, F.B., N. Lai, J.H. Trainor, M.A.I. Van Hollebeke and W.R. Webber, The solar modulation of galactic cosmic rays in the outer heliosphere, Astrophys. J., 249, L71, 1981.

McDonald, F.B., J.H. Trainor, J.D. Mihalov, J.H. Wolfe, and W.R. Webber, Radically propagating shock waves in the outer heliosphere: The evidence from Pioneer 10 energetic particle and plasma observations, Astrophys. Lett., 246, 2165, 1981.

McKibben, R.B., K.R. Pyle and J.A. Simpson, The galactic cosmic-ray radial gradient and large-scale modulation in the heliosphere, Astrophys. J., 254, L23, 1982.

Newkirk, G. Jr., A. J. Hundhausen and V. Pizzo, Solar cycle modulation of galactic cosmic rays: speculation on the role of coronal transients, J. Geophys. Res., 86, 5387, 1981.

Perko, J.S. and L.A. Fisk, Solar modulation of galactic cosmic rays: 5. time-dependent modulation, J. Geophys. Res., 88, 9033, 1983.

Pyle, K.R., J.A. Simpson, J.D. Mihalov and J.H. Wolfe, Large-scale modulation of galactic cosmic-rays and anomalous H_e observed at 16 au with Pioneer 10, Proc. Intl. Conf. Cosmic Rays 16th, 5, 345, 1979.

Smith, E.J., The magnetic field in the outer heliosphere, EOS, 63, 1053, 1982.

Smith, E.J., L. Davis, Jr., P.J. Coleman, Jr., D.S. Colburn, P. Dyal and D.E. Jones, August 1972 solar-terrestrial events: observations of interplanetary shocks at 2.2 au, J. Geophys. Res., 82, 1077, 1977.

Smith, E.J. and J.H. Wolfe, Fields and plasma in the outer solar system, Space Sci. Rev., 23, 1979.

Thomas, B.T. and E.J. Smith, The structure and dynamics of the heliospheric current sheet, J. Geophys. Res., 86, 11105, 1981.

Van Allen, J.A., Galactic cosmic-ray intensity from 1 to 9 au, Geophysical Res. Lett., 3, 425, 1976.

Webber, W.R. and J.A. Lockwood, Study of the long-term variation and radial gradient of cosmic rays out to 23 au, J. Geophys. Res., 86, 11458, 1981.

- Wu, S.T., Theoretical interpretation of traveling interplanetary phenomena and their solar origins, p. 443 in Solar and Interplanetary Dynamics, ed. by M. Dryer and E. Tandberg-Hanssen, D. Reidel Pub. Co., Dordrecht-Holland, 1980.
- Wu, S.T., Y. Nakagawa and M. Dryer, dynamic modeling of coronal and interplanetary responses to solar events, p. 43, in Study of Travelling Interplanetary Phenomena, 1977, ed. by M.A. Shea, D.F. Smart and S.T. Wu, D. Reidel Pub. Co., Dordrecht-Holland, 1977.
- Wu, S.T., S.M. Han and M. Dryer, Two-dimensional, time-dependent MHD description of interplanetary disturbances: simulation of high speed solar wind interactions, Planet. Space Sci., 27, 255, 1979.
- Wu, S.T., M. Dryer and S.M. Han, Non-planar MHD model for solar flare-generated disturbances in the heliospheric equatorial plane, Solar Phys., 84, 395, 1983.

Table 1

Solar radio
(Peak)
8800 MHz
Flare ($\times 10^{-22}$
Imp W/m^2 Hz)

active
region
ssc

Location

UT

Flare
Imp

Location

active
region
ssc

	UT	Flare Imp	Solar radio (Peak) 8800 MHz Flare ($\times 10^{-22}$ Imp W/m^2 Hz)	Location	CMP	active region ssc
1	June 3	1141	2B 6000	S12 E72	8.89	A June 6 0244
	June 5	0655	3B 1742	S12 E43	8.53	A
		0729	3B 1321	S08 E46	8.76	A
2	June 6	1630	3B 3500	S09 E25	8.57	A June 9 0040
	June 7	0826	3B 579	S10 E13	8.33	A
3	June 10	0059	2B 1174	S10 W22	8.39	A June 12 1443
4a	(June 16)	(0000)	—	(S10)(L152)	(8.39)	(A)
	June 20	0151	2B 3539	N14 W17	18.79	
	June 23	0628	3B 59	N17 W30	20.99	B
4b	(July 1)	(0000)	—	(N15) (L132)	(20.99)	(D) (July 5)
5	July 9	0730	3B 5700	N16 E77	15.16	C July 11 0953
6	July 12	0910	3B 6200	N12 E39	15.32	C July 13 1617
						Intense geomagnetic storm and Forbush decrease
7	July 14	1313	2B 50	N12 E21	16.16	C July 16 1519

Table 2

	Month	Day	*T _F (hr)	Longitude (in heliographic coordinate)	Latitude	V _F	τ	σ	α
Flare 1	6	3	376.7	302.4	-12.0	820	5.0	80°	240
Flare 2	6	6	453.5	352.2	- 9.0	560	5.0	50°	240
Flare 3	6	10	534.0	43.1	-10.0	520	5.0	30°	240
Flare 4a	6	20	773.0	182.4	-10.0	1700	10.0	15°	1000
Flare 4b	7	1	1049.0	173.0	15.0	600	5.0	70°	1000
Flare 5	7	9	1236.5	330.9	16.0	1520	10.0	80°	240
Flare 6	7	12	1310.2	12.8	12.0	2120	10.0	80°	240
Flare 7	7	14	1362.2	32.4	12.0	580	10.0	80°	240

*T_F = 0 corresponds to the beginning time of Carrington rotation 1722.

Table 3

McMath							
Plage							
Date	Flare	Location	Number	Importance		ssc	
1	April 8, 1978	0109	N19 W11	15221	2B	April 10	1306 UT
2	April 11, 1978	1334	N22 W56	15221	2B	April 13	1925
3	April 17	1200	(unobserv)	15266			
4	April 28	1304	N22 E38	15266	3B	April 30	1925
5	April 29	2010	N20 E14	15266	2B	May 1	0828
6	April 30	1420	N28 E14	152166	3B	May 1	1835
7	May 1	1910	N21 W12	15266	2B	May 2	2318

Table 4

	Date	FLR(T)	Longitude	Latitude	V	τ	σ	τ_F
1	April 8	0.0	32.7	19.0	450.0	10.0	30.0	1000.0
2	April 11	84.4	80.7	22.0	800.0	10.0	60.0	1000.0
3	April 15	(226.8	210.6	22.0)	400.0	10.0	95.0	1000.0
4	April 28	491.9	3.3	22.0	580.0	20.0	190.0	1000.0
5	April 29	523.0	28.3	20.0	900.0	10.0	60.0	1000.0
6	April 30	541.2	29.2	28.0	1300.0	10.0	60.0	1000.0
7	May 1	570.0	56.2	21.0	1100.0	10.0	90.0	1000.0

Table 5

Time	Event at Pioneer 10	Event at Pioneer 11
6/6-7		Solar Protons
6/24-28	CIR (model)	
7/1		Vsw transient from flares 1 (model)
7/2-3		Small increase in Vsw
7/3-12		Cosmic ray decrease
7/6		Vsw transient from flares 2 (model)
7/7-10	CIR (model)	
7/9-10		Small increase in Vsw
7/20-22	CIR (model)	
7/25-26		Small increase in Vsw
7/26		CIR arrival (model)
7/29-30	Transient from flare 4a Step increase in Vsw	
7/30-8/3	Cosmic ray decrease	
8/1-3	CIR (model)	
8/3		Vsw transient from flares 5 & 6 (model) Step increase in Vsw
8/7-9		Cosmic ray decrease
8/14-17	CIR (model)	

Figure Captions

- Figure 1. Hydrogen-Alpha synoptic charts for Carrington Rotations 1722, 1723 and 1724 from Solar-Geophysical Data, no. 455, 456, 457 and 458. The three active regions, A, B and C are indicated.
- Figure 2. Hydrogen-Alpha filtergram profiles near central meridian passage time of the three regions A, B and C (Solar-Geophysical Data, no. 455, 456, 457, 458).
- Figure 3. Satellite situation charts at the time of the 8 flares. The locations of the flare, Venus (Pioneer 12), Earth, Pioneers 10, and 11 are shown at 00UT on each flare date. Note that in this figure only, the radial distance is given on a logarithmic scale in astronomical units (au) (A. Barnes, private communication).
- Figure 4. Solar speed observed at Pioneer 10, 11 and 12 and the magnetic field magnitude observed at ISEE-3 for the period 20 June to 20 August, 1982 (E. J. Smith, private communication).
- Figure 5. Energetic particle Cherenkov Detector data at Pioneer 10 and 11, and the Deep River neutron monitor record during the period between 1980 and 1983 (W. Fillius and W. I. Axford, 1984).
- Figure 6a. Frame 1 and 2 show the background velocity distribution in heliographic coordinates (fixed on the source surface of 2.5 solar radii) and the contribution to the velocity distribution due to flare #1, respectively. The third frame shows the time dependence of the particle velocity for flare #1. See text for details.

- Figure 6b. Solar wind speed distribution at maximum epoch for the eight flares in Table 2.
- Figure 7a-f. Equatorial plane projections of solar wind disturbances in the inner heliosphere (to 2 au) caused by the six flares 1, 2, 3, 5, 6, 7 at the time of shock arrival at the earth.
- Figure 8a-b. Equatorial plane projections of solar wind disturbances in the outer heliosphere (to 30 au) caused by the six flares 1, 2, 3, 5, 6, 7 at $T = 1752$ hr. (73.0 day, July 30), and $T = 1848$ hr. (77.0 day, August 3), respectively. The location of Pioneer 10 (~28 au) in Figure 8a and Pioneer 11 (~12 au) in Figure 8b are indicated by the * mark.
- Figure 9a-b. Equatorial plane solar wind disturbances at $T = 1133$ hr (47.2 day, July 5) with flare 4b included. Plots are shown out to 2 au and 5 au respectively.
- Figure 10a-d. Equatorial plane solar wind disturbances at $T = 1437$ hr (59.9 day, July 17), 1651 hr (68.8 day, July 26), 1752 hr (73.0 day, July 30) and 1848 hr (77.0 day, August 3) with flares 4a and 4b included.
- Figure 11. Simulated solar wind bulk speed at Pioneer 10, 11 and 12 and IMF magnitude at ISEE-3 for the period 20 June to 20 August, 1982. Compare this figure tes in Table 2.
- Figure 12. Satellite situation charts at the time of the 7 flares. The locations of the flare, Earth, Pioneers 10 and 11 are shown at 00UT on each flare date. Note that the radical distance is given on a logarithmic scale in astronomical units (au).




Figure 13.

Equatorial plane projections of solar wind disturbance in the inner heliosphere (to 2 au) caused by the six flares, 1, 2, 4, 5, 6, 7 at the time of shock arrival at the earth.

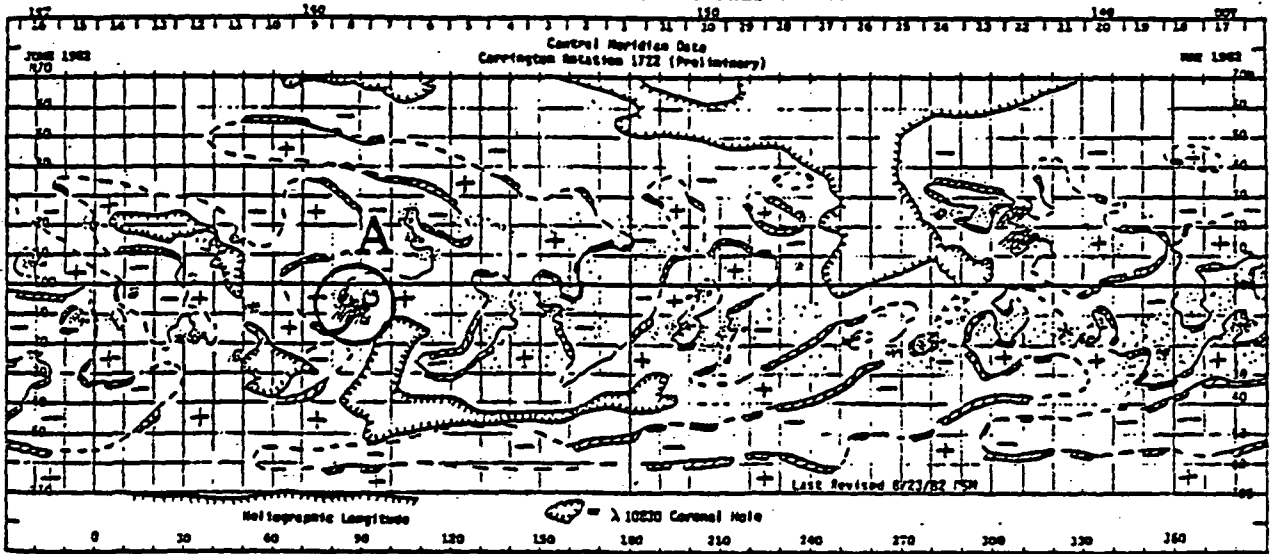
Figure 14.

Equatorial plane projections of solar wind disturbance in the outer heliosphere on May 8, 11, 27 and June 5. The locations of Pioneers 10 and 11 are indicated.

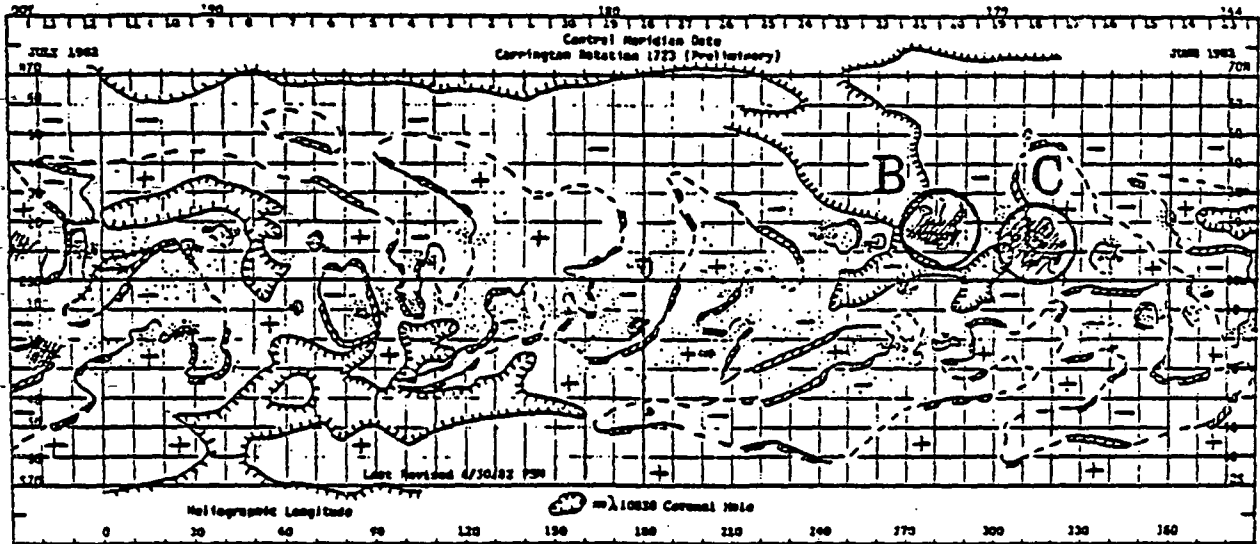
Figure 15.

Observed and simulated solar wind bulk speed at Pioneers 10 and 11. The observed speed is taken from Intriligator and Miller (1982).

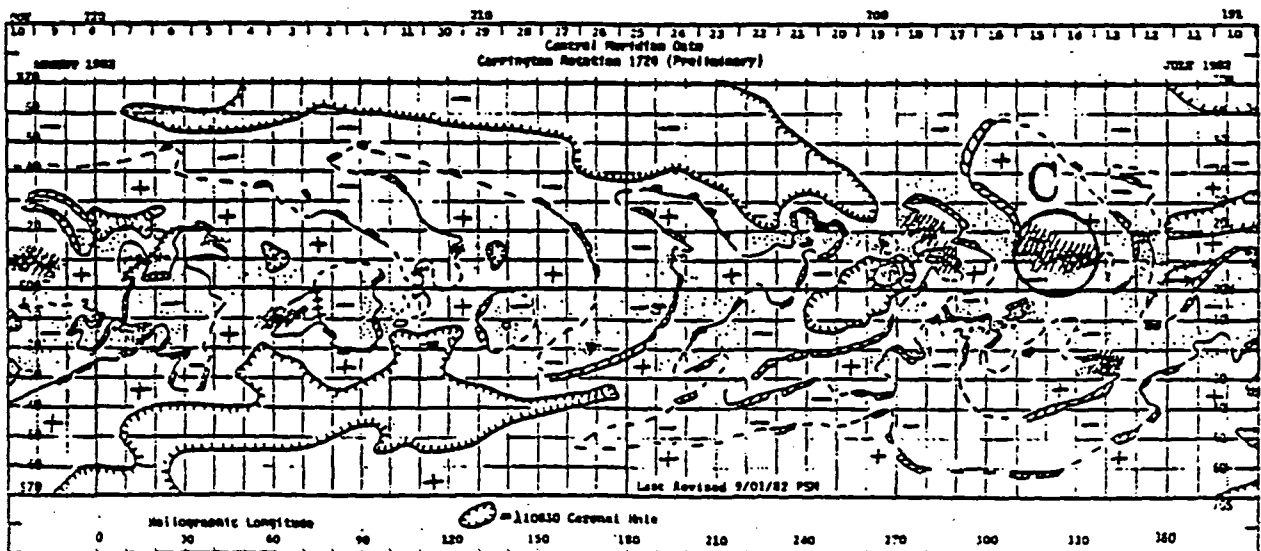
He SYNOPTIC CHART
CARRINGTON ROTATION 1722 (PRELIMINARY)



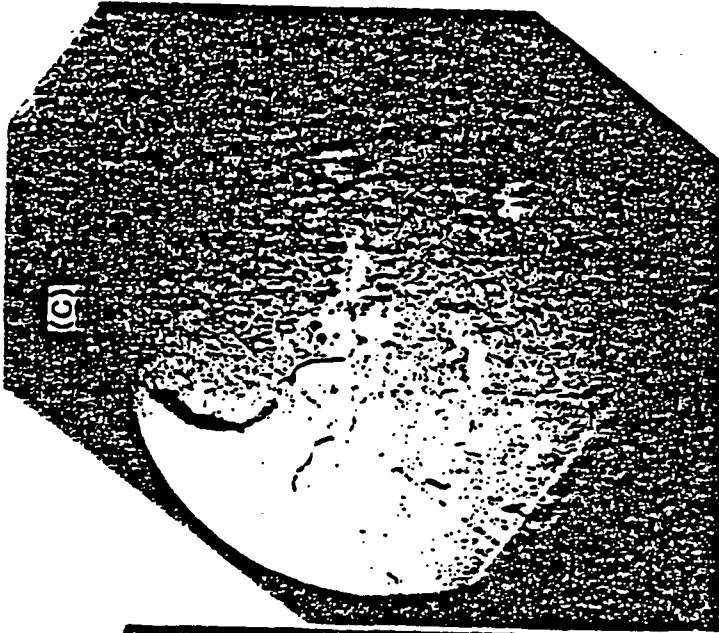
He SYNOPTIC CHART
CARRINGTON ROTATION 1723 (PRELIMINARY)



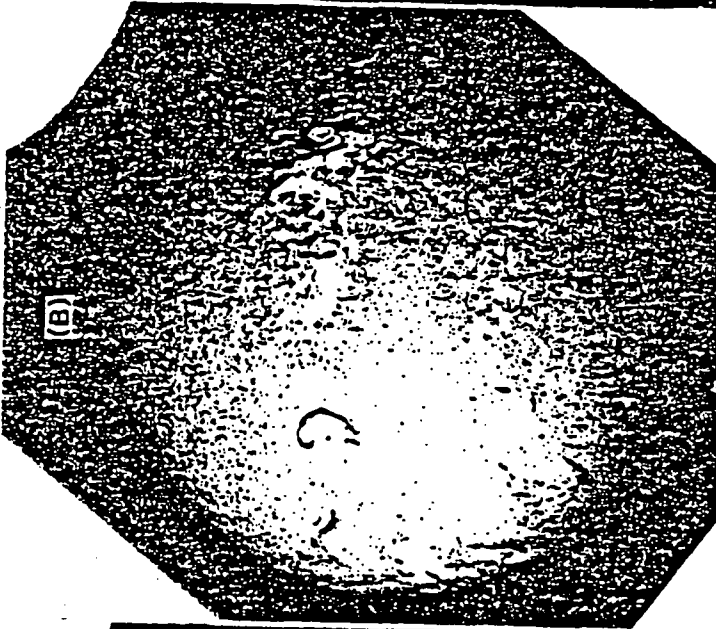
He SYNOPTIC CHART
CARRINGTON ROTATION 1726 (PRELIMINARY)



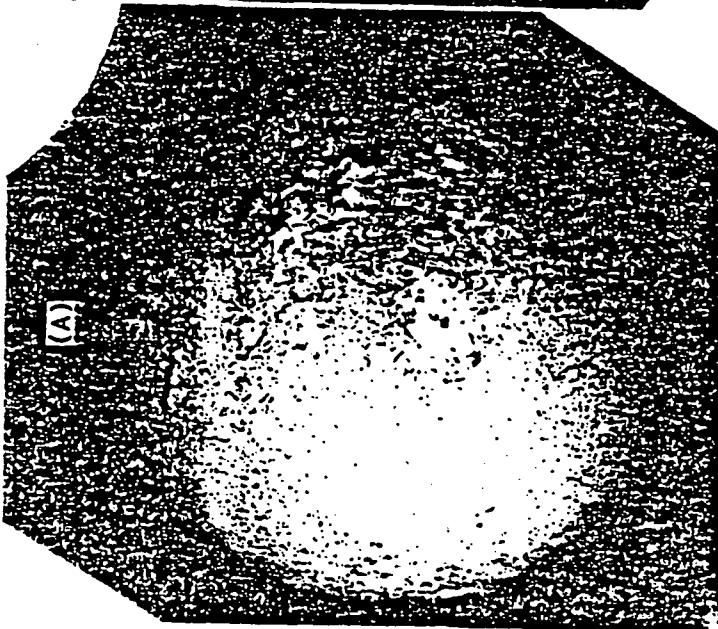
ORIGINAL PAGE IS
OF POOR QUALITY



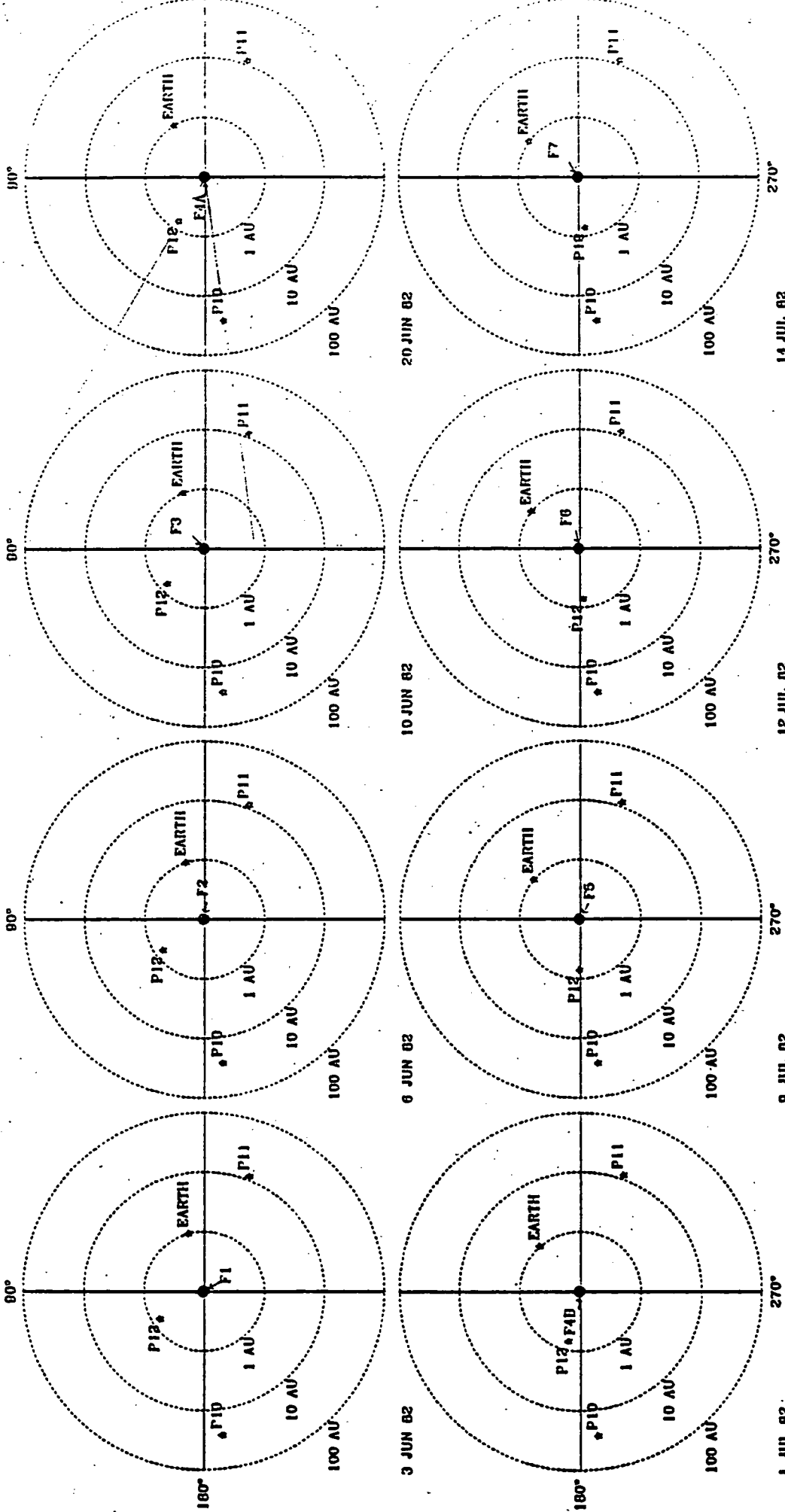
JUNE 15, 1982
1430



JUNE 21, 1982
1632

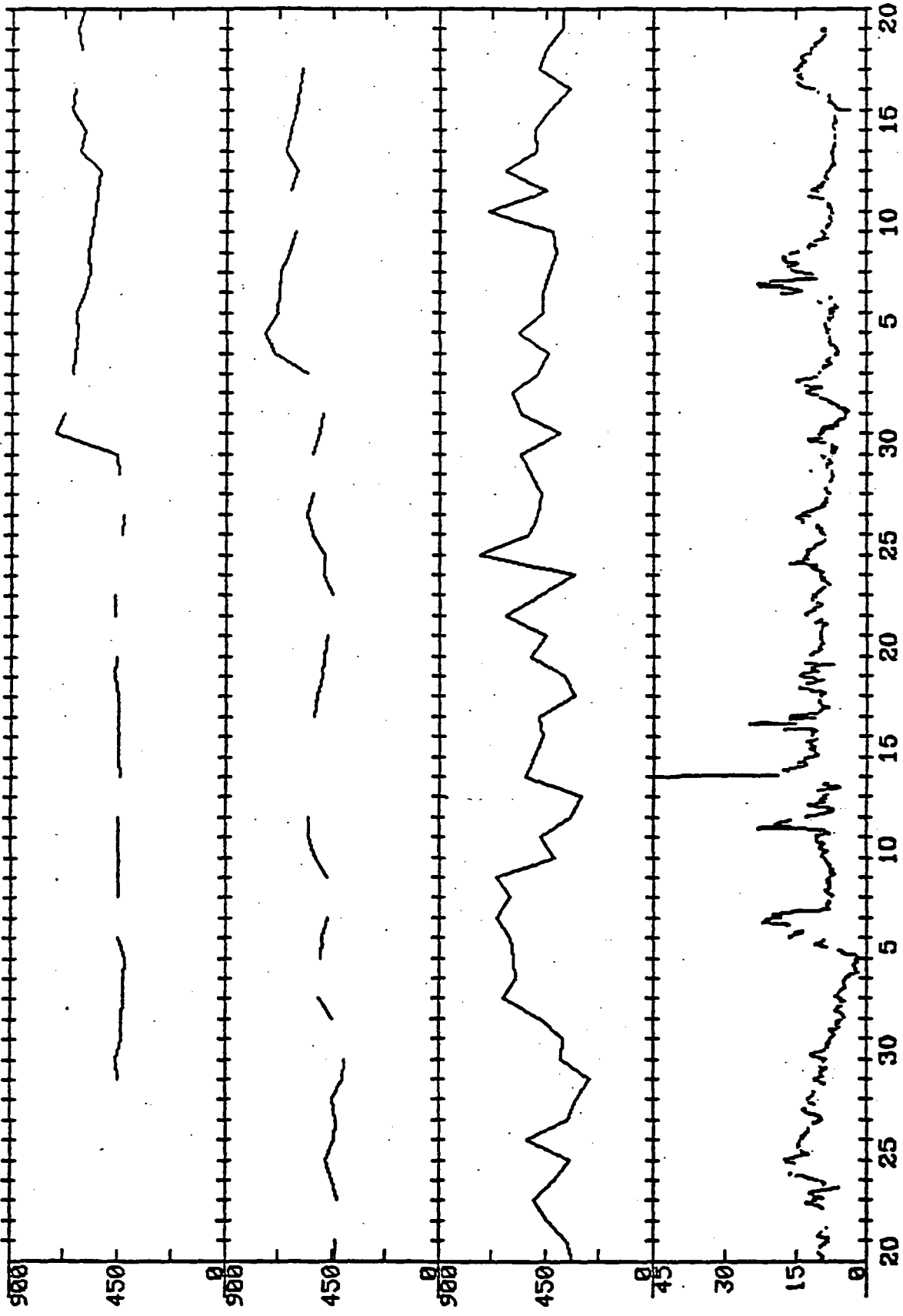


JUNE 8, 1982
1450



SOLAR WIND VELOCITY

PION 10 PION 11 PION 12 /B/ ISEE-3 GARMAS

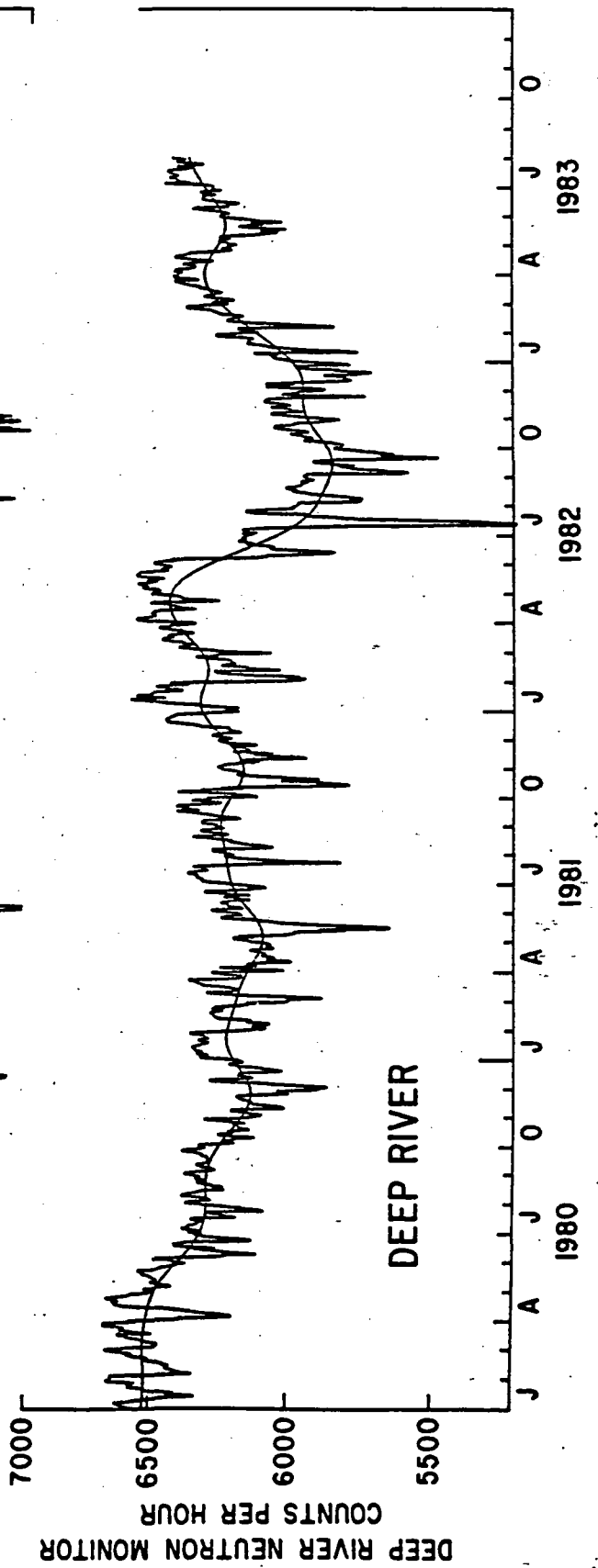
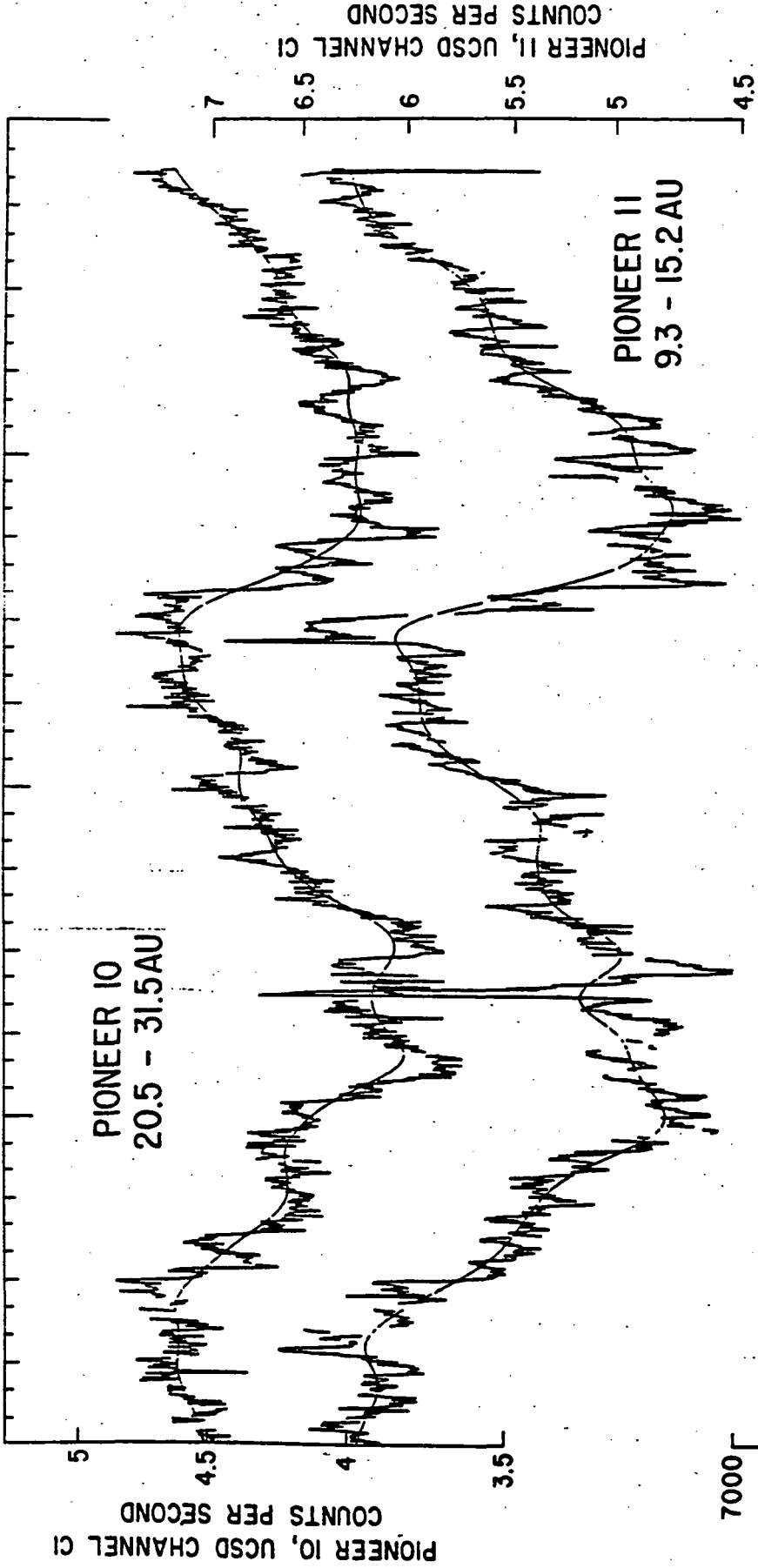


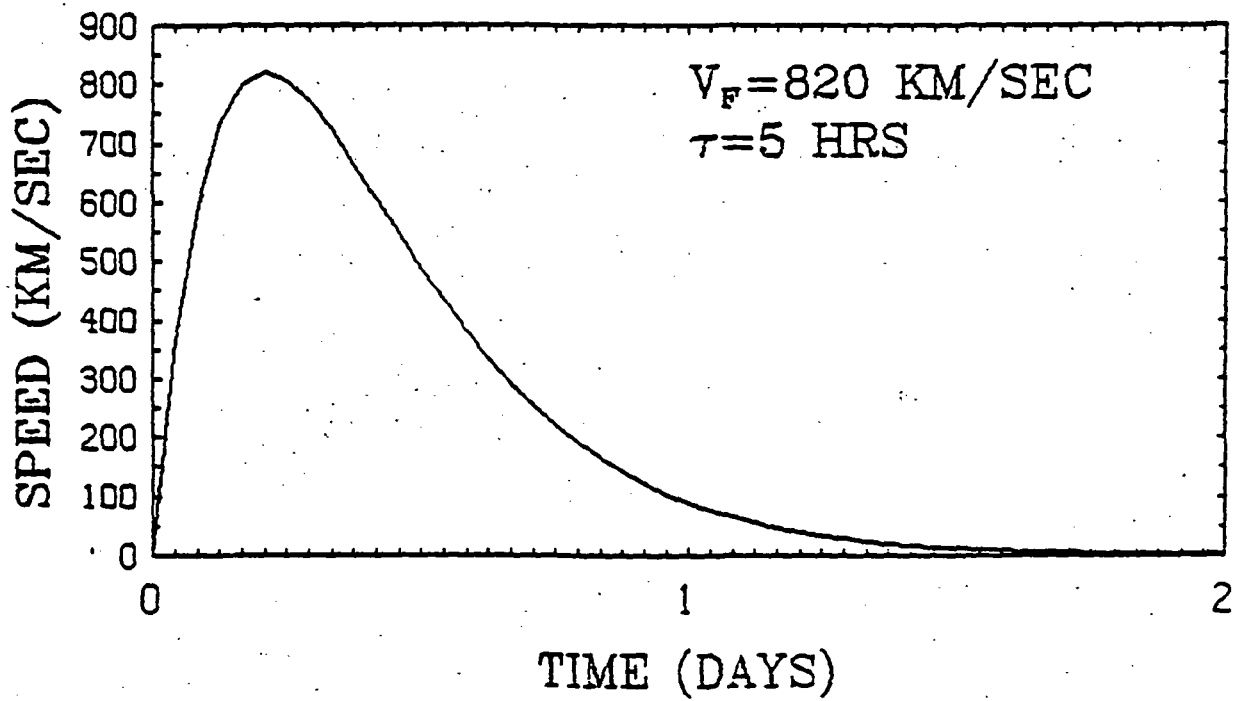
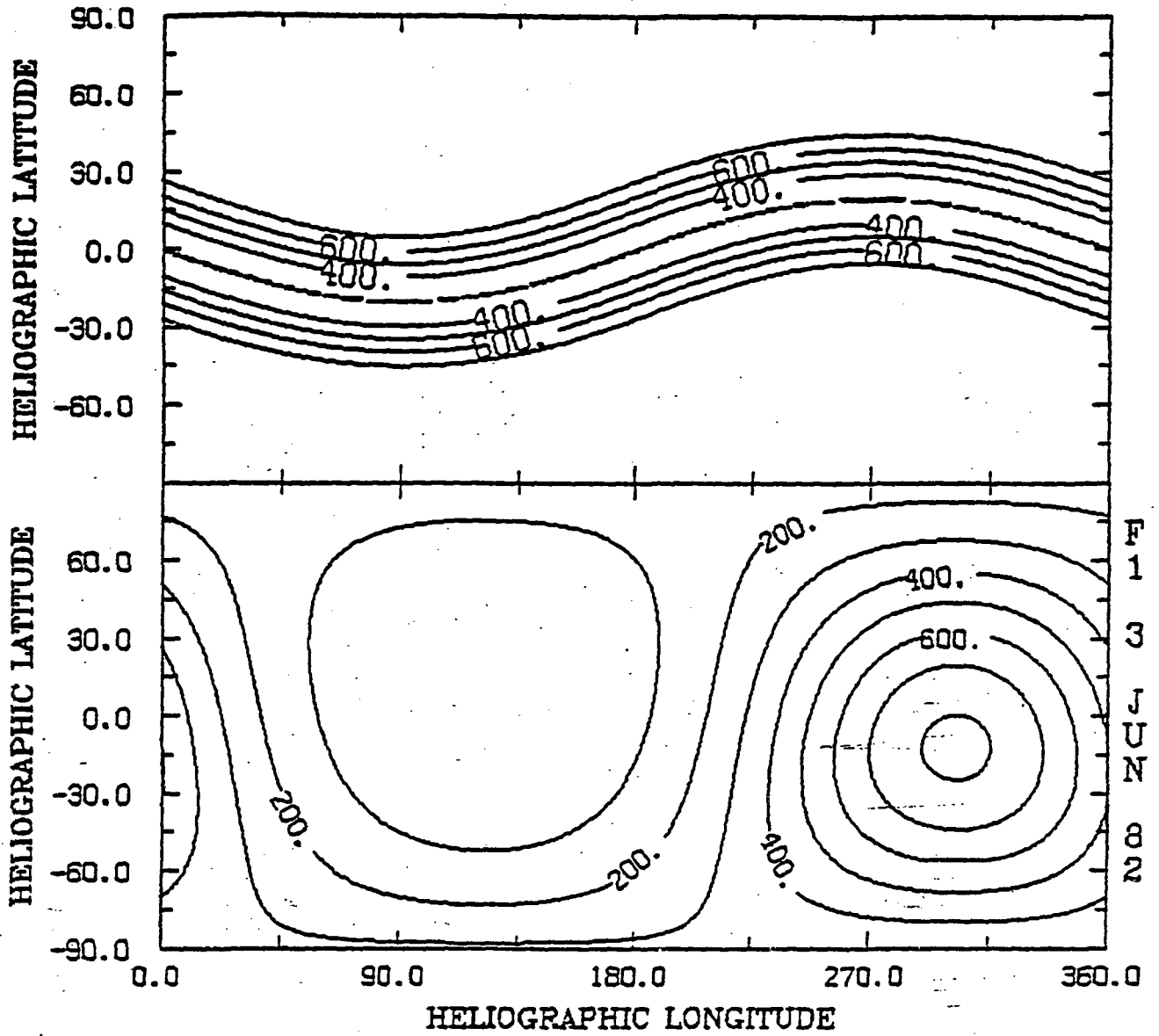
AUG.

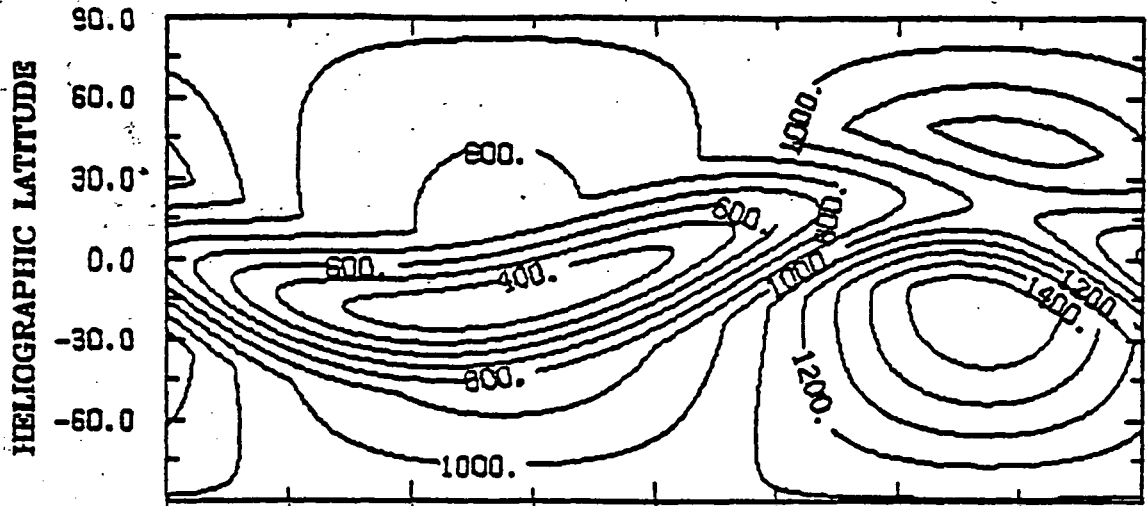
JULY

JUNE

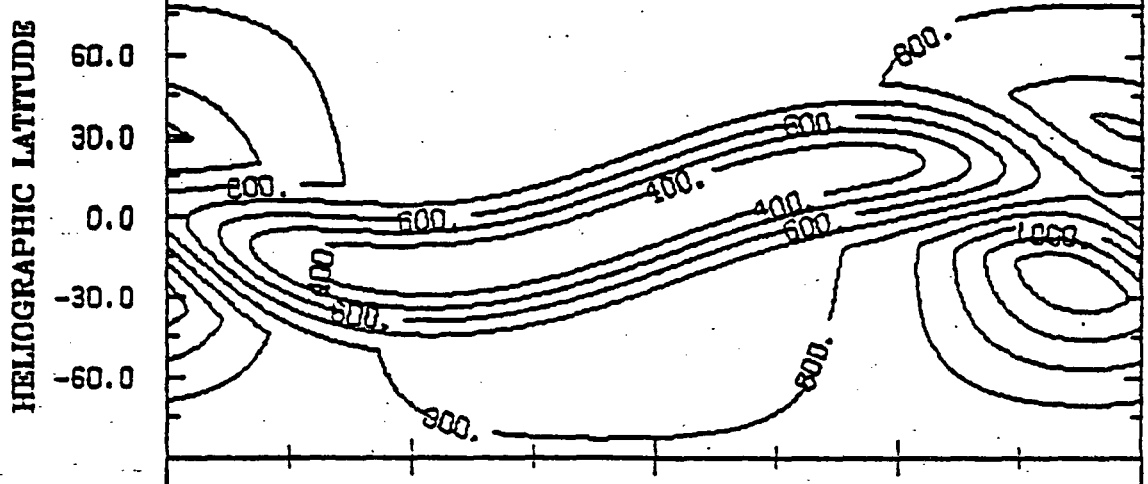
1982



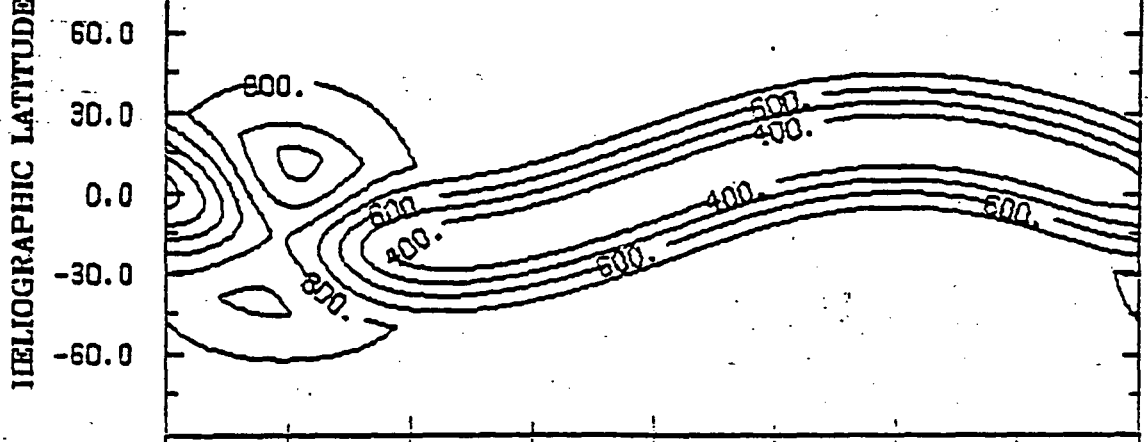




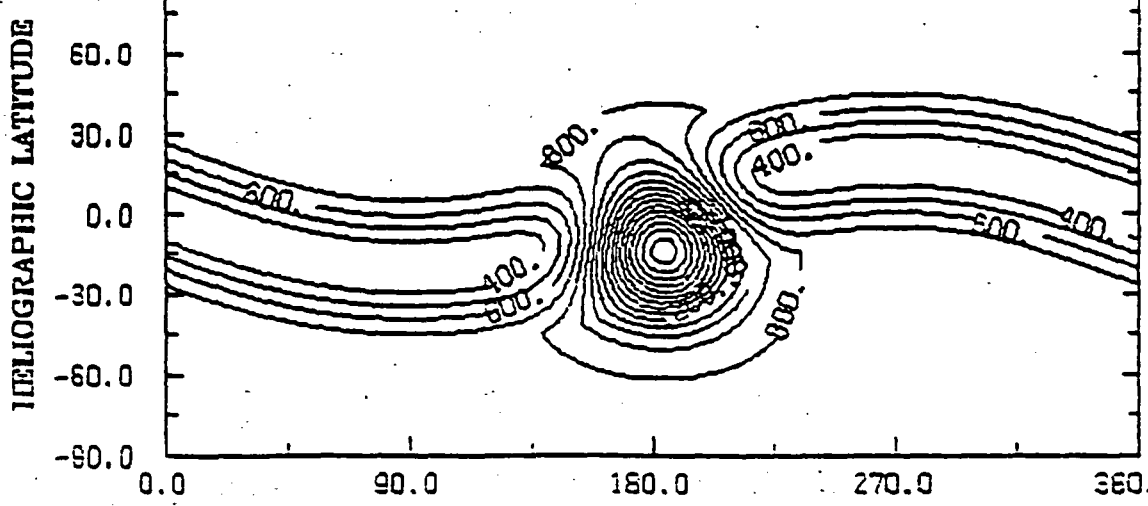
F1
3
JUNE
1982



F2
6
JUNE
1982



F3
10
JUNE
1982



F4A
20
JUNE
1982

90.0
60.0
30.0
0.0
-30.0
-60.0
-90.0

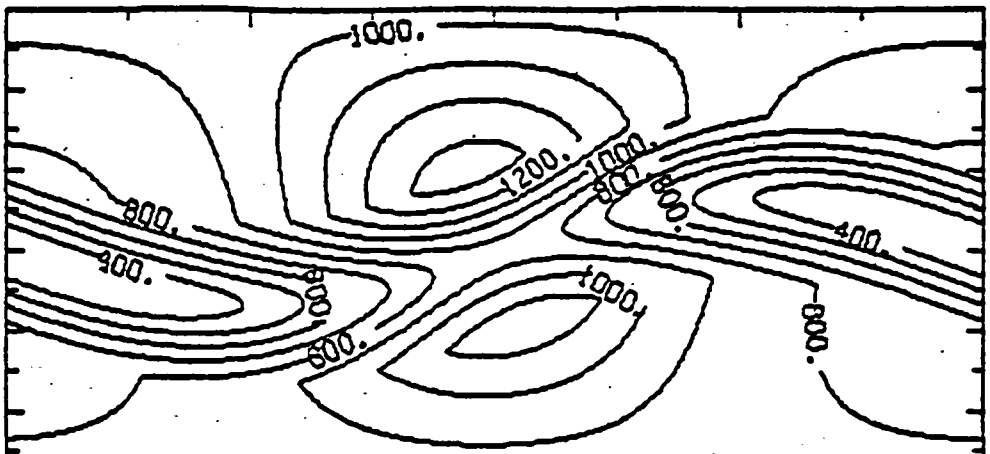
0.0 90.0 150.0 270.0 360.0

HELIOGRAPHIC LATITUDE

HELIOGRAPHIC LONGITUDE

HELIOGRAPHIC LATITUDE

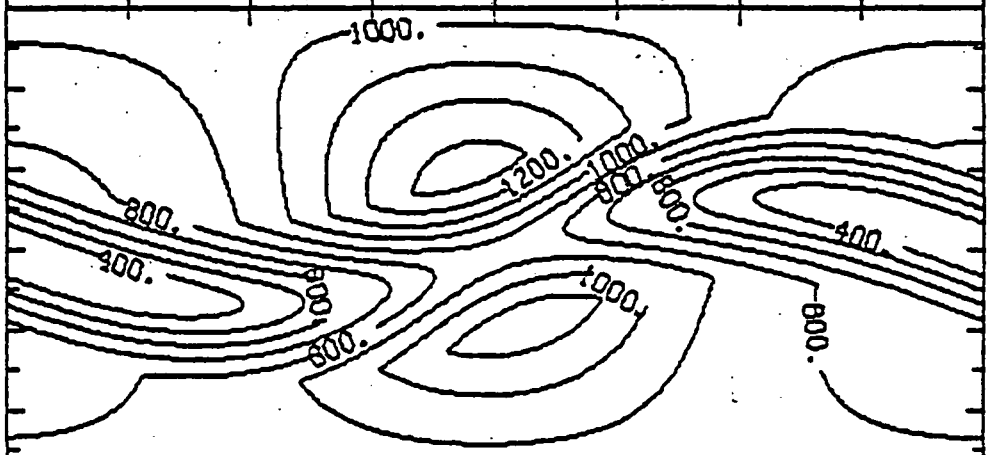
90.0
60.0
30.0
0.0
-30.0
-60.0



F4B
1
JULY
1982

HELIOGRAPHIC LATITUDE

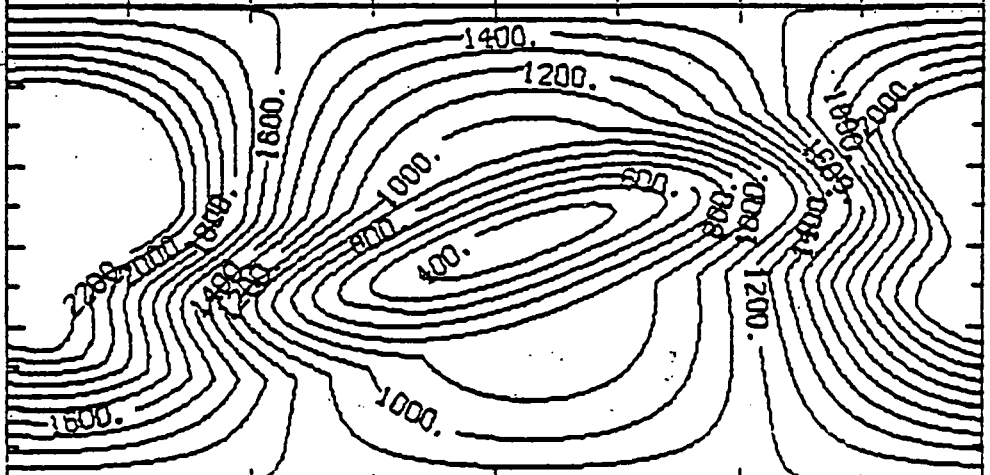
60.0
30.0
0.0
-30.0
-60.0



F5
9
JULY
1982

HELIOGRAPHIC LATITUDE

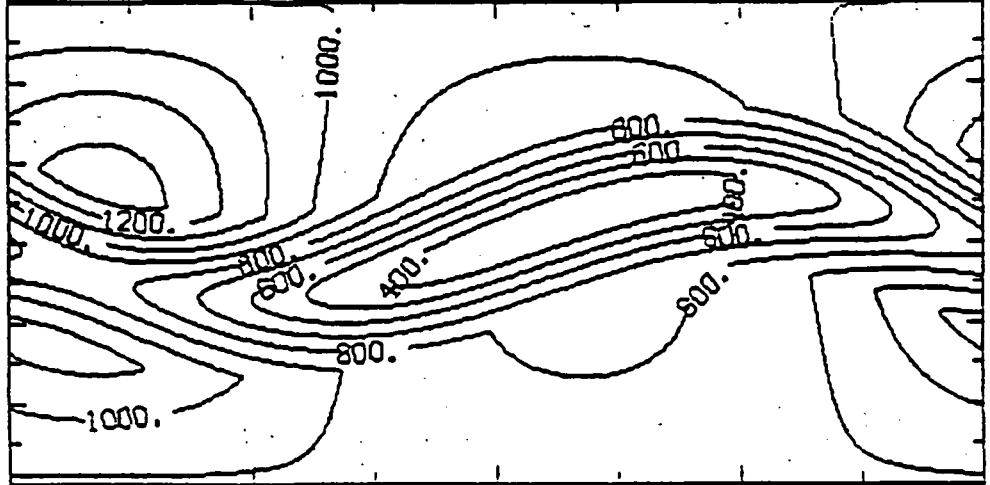
60.0
30.0
0.0
-30.0
-60.0



F6
12
JULY
1982

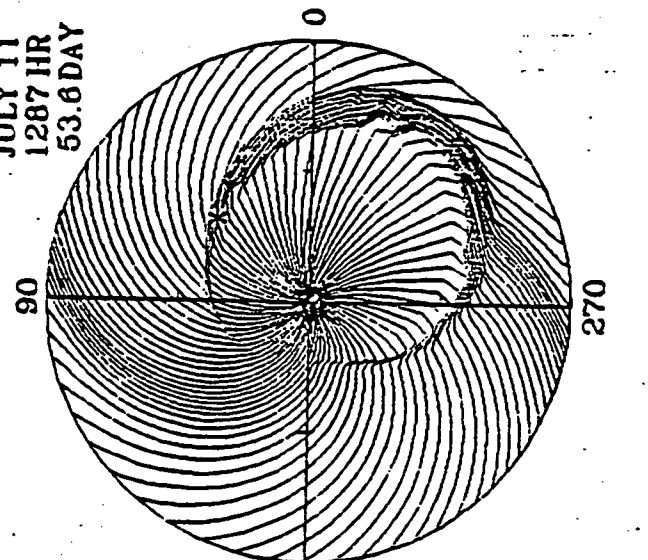
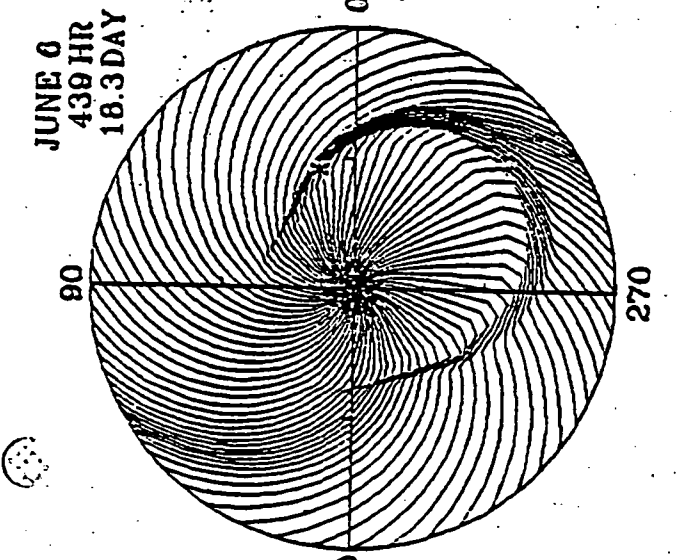
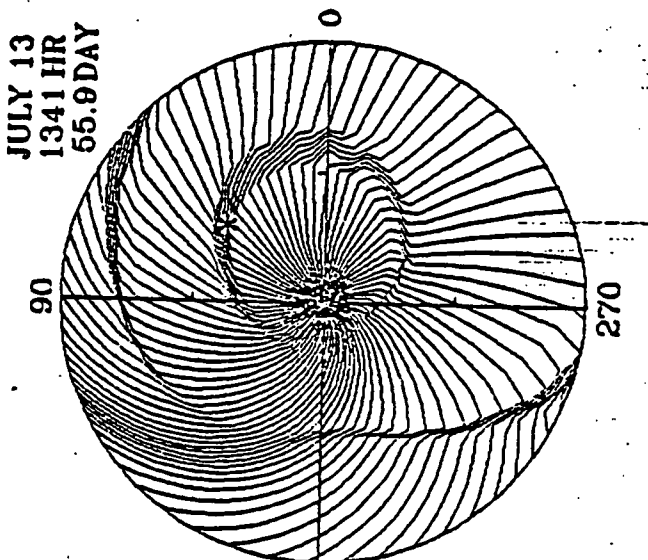
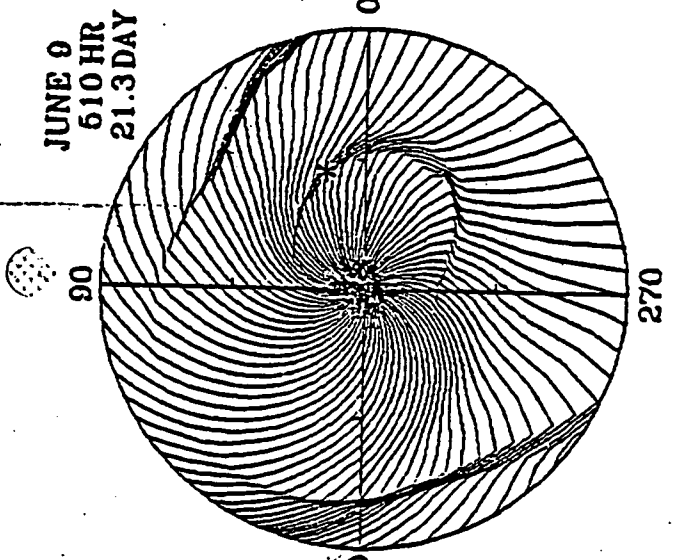
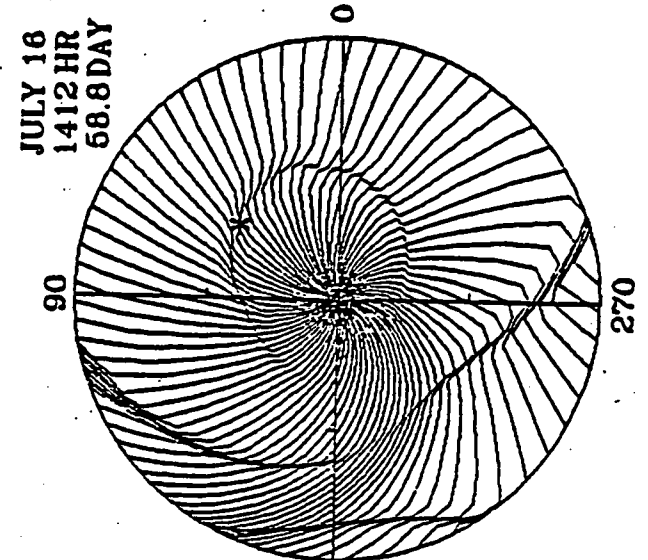
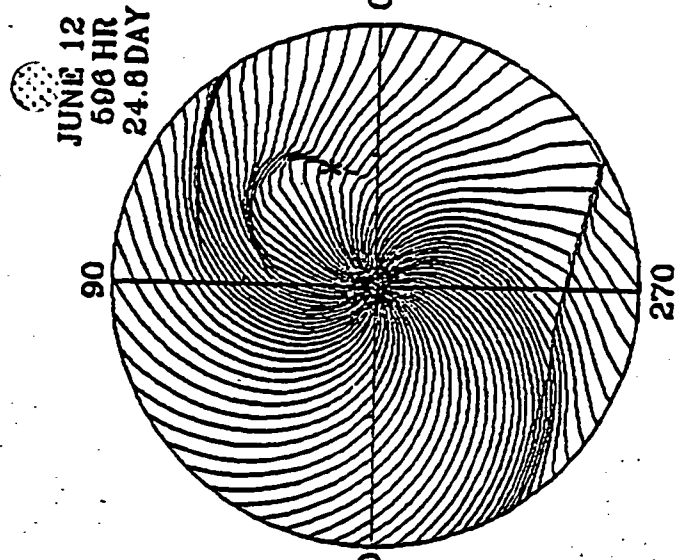
HELIOGRAPHIC LATITUDE

60.0
30.0
0.0
-30.0
-60.0
-90.0



F7
14
JULY
1982

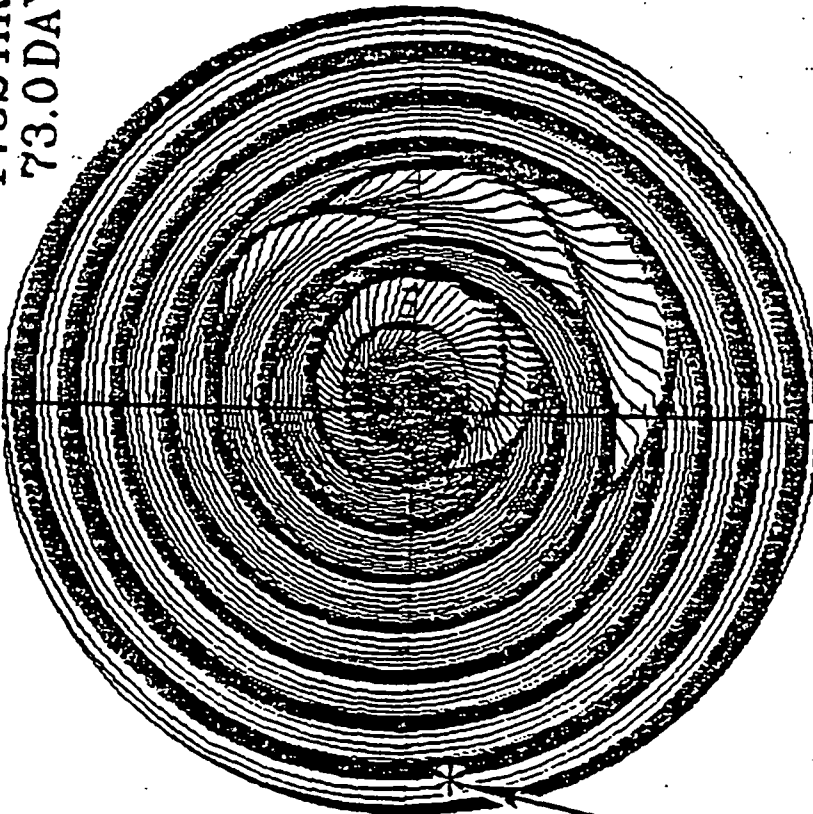
0.0 90.0 180.0 270.0 360.0
HELIOGRAPHIC LONGITUDE



* EARTH
EQUATORIAL PLANE

JULY 30
1752 HR
73.0 DAY

90

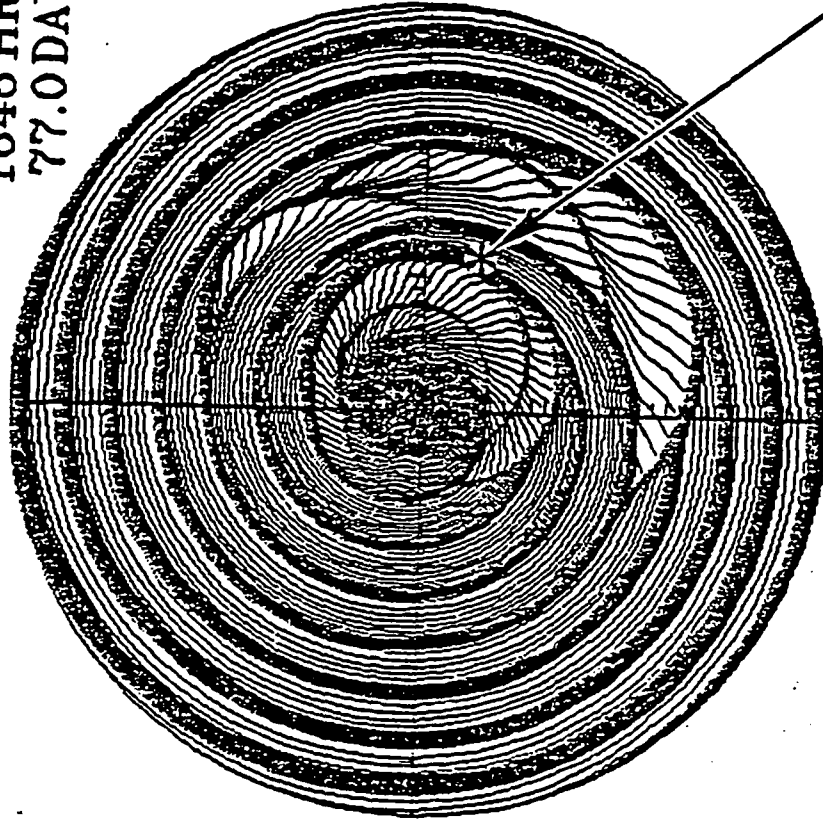


180

Pioneer 10 270

AUG 3
1848 HR
77.0 DAY

90



0 180

270 Pioneer 11

ORIGINAL IMAGE IS
OF POOR QUALITY

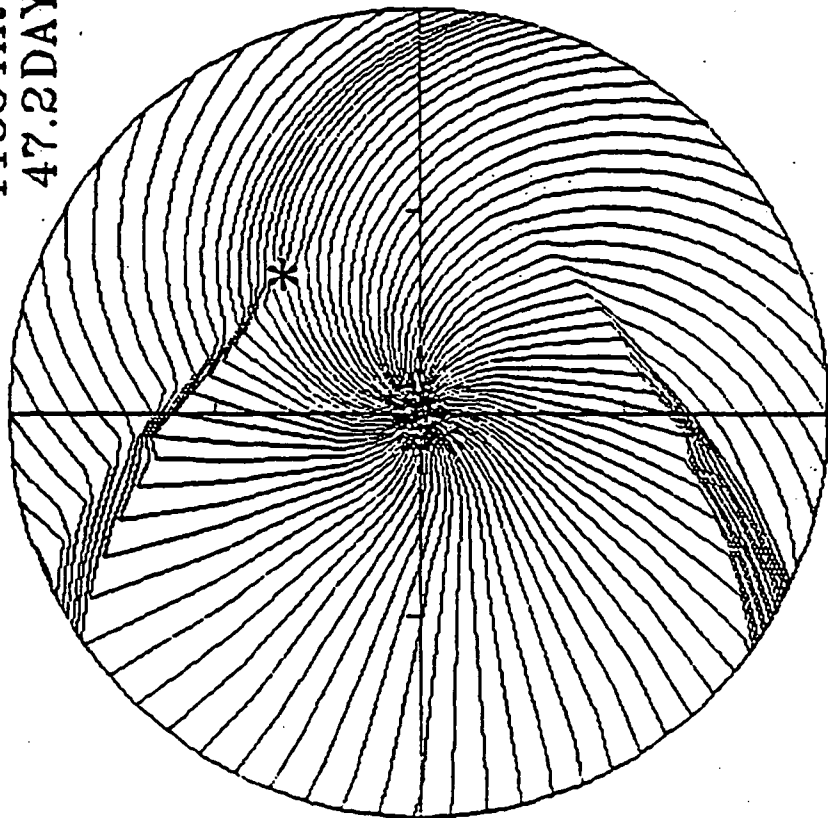
EQUATORIAL PLANE

Fig. 8a-b

JULY 5
1133 HR
47.2 DAY

2AU

90



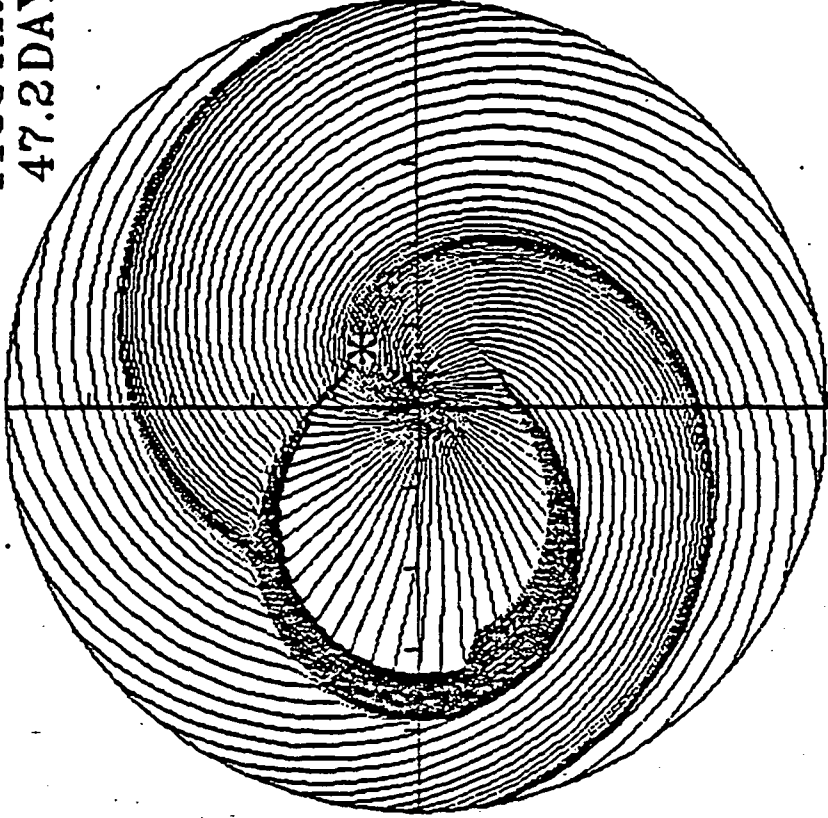
270

(A)

5AU

JULY 5
1133 HR
47.2 DAY

90



270

(B)

EQUATORIAL PLANE

ORIGINAL PAGE IS
OF POOR QUALITY

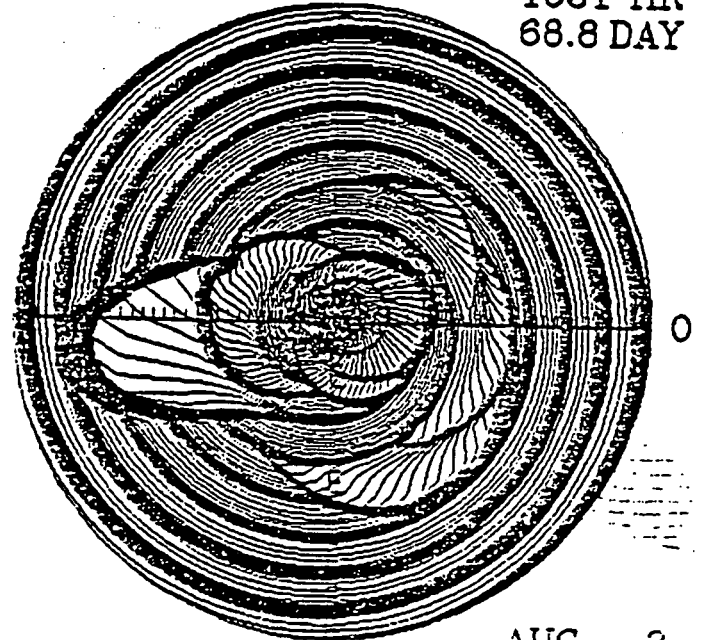
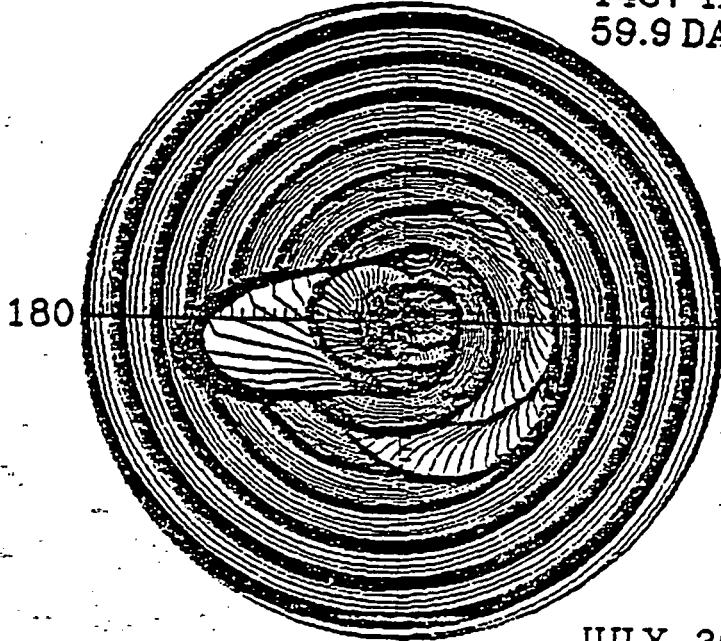
30 AU

90

JULY 17
1437 HR 30 AU
59.9 DAY

90

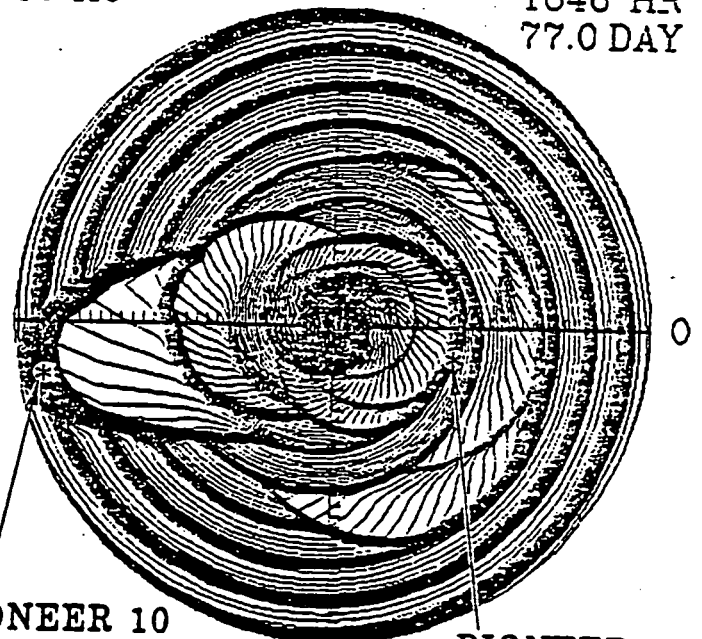
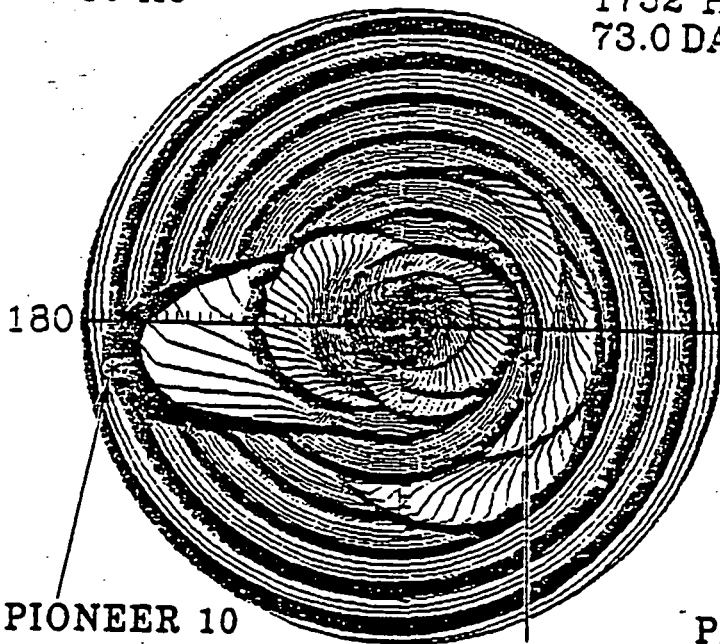
JULY 26
1651 HR
68.8 DAY



30 AU

JULY 30
1752 HR 30 AU
73.0 DAY

AUG 3
1848 HR
77.0 DAY



PIONEER 10

270

PIONEER 11

PIONEER 10

270

PIONEER 11

EQUATORIAL PLANE

SIMULATED PARAMETERS
/B/
SOLAR WIND VELOCITY

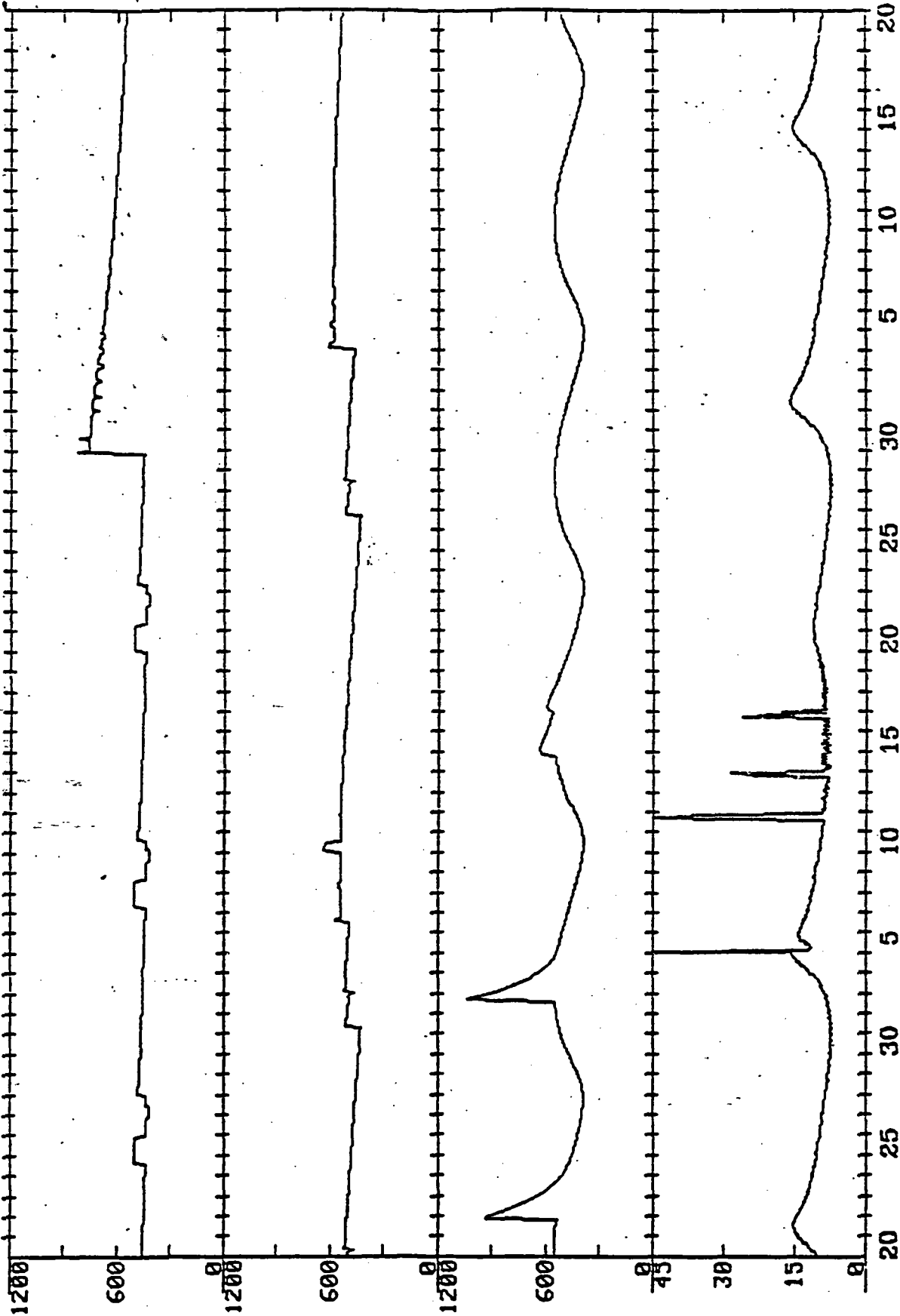
PION 10 PION 11 PION 12

KM/SEC

KM/SEC

KM/SEC

GAMMAS



AUG.

JULY

1982

JUNE

Fig. 11

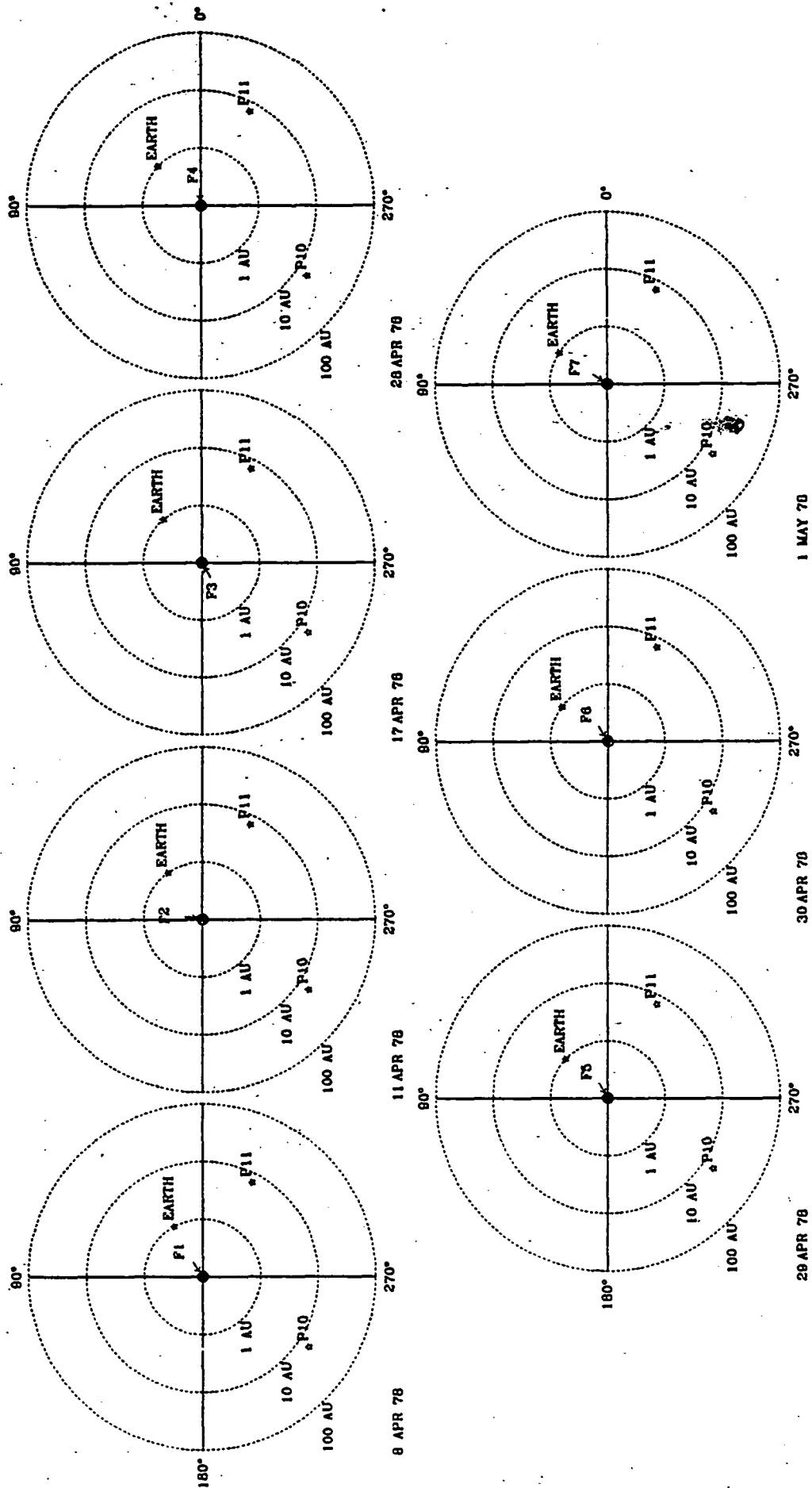
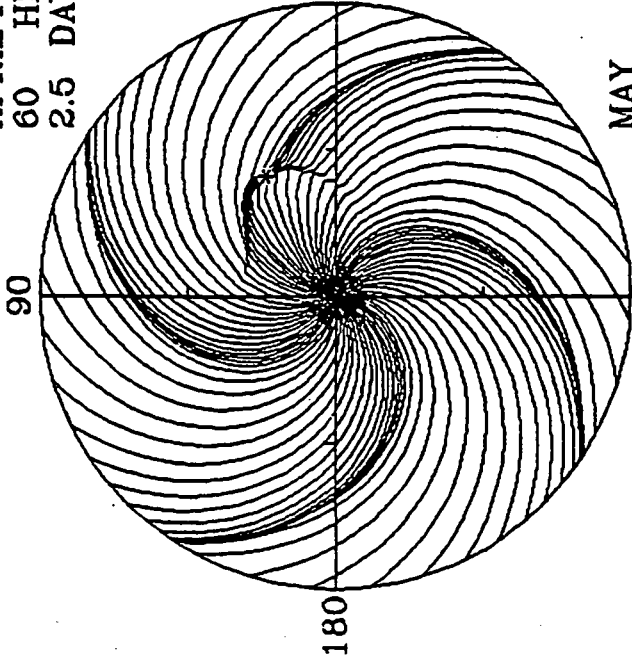
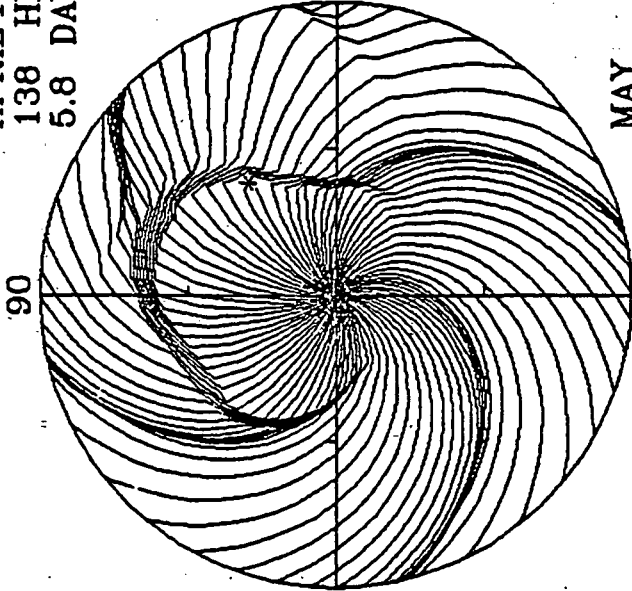


FIG. 12

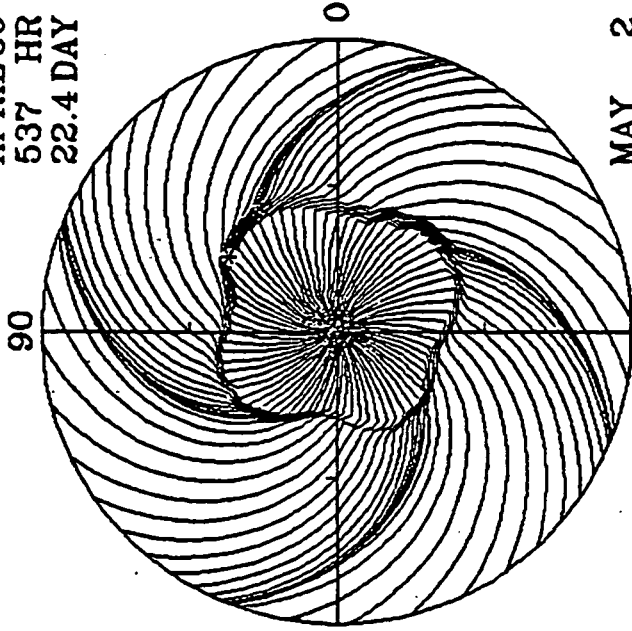
APRIL 10
60 HR
2.5 DAY



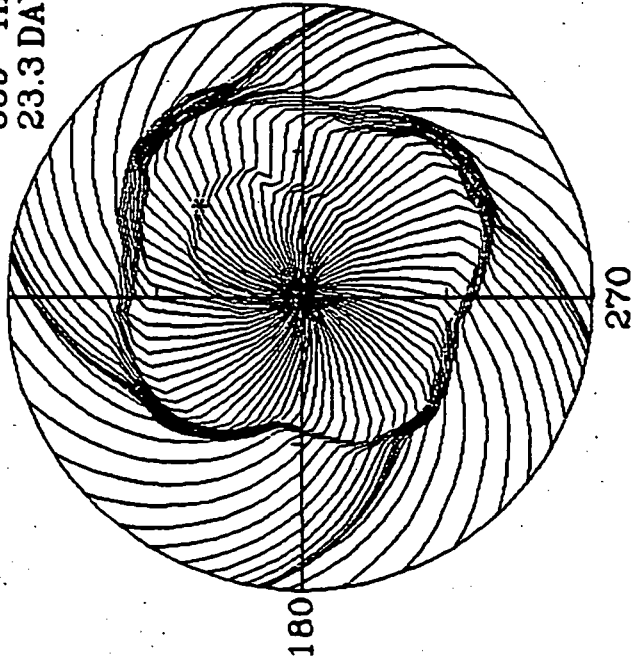
APRIL 13
138 HR
5.8 DAY



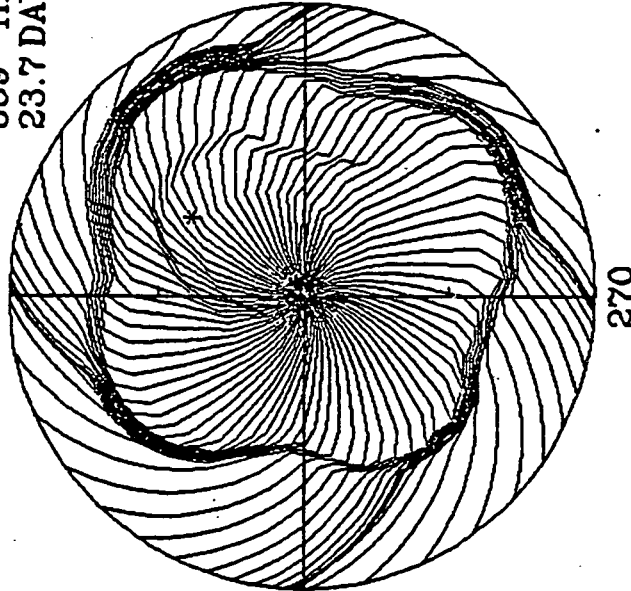
APRIL 30
537 HR
22.4 DAY



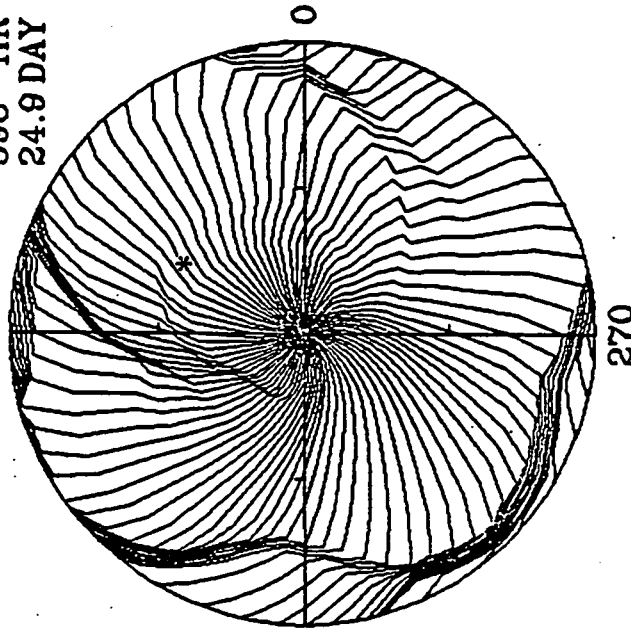
MAY 1
559 HR
23.3 DAY



MAY 1
569 HR
23.7 DAY



MAY 2
598 HR
24.9 DAY



(* EARTH)
EQUATORIAL PLANE

Fig. 13

ORIGINAL PAGE IS
OF POOR QUALITY

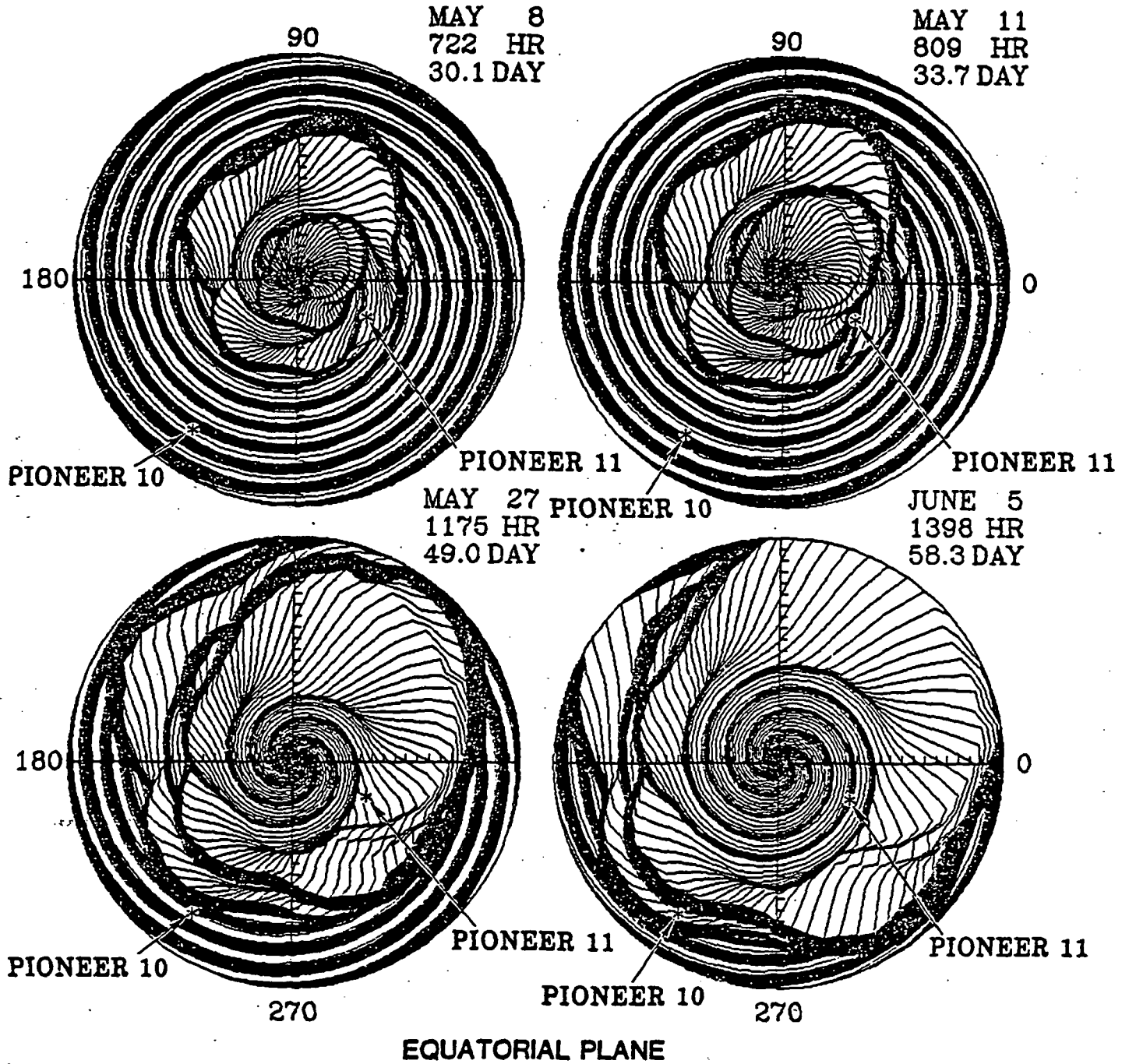


Fig. 14

ORIGINAL PAGE IS
OF POOR QUALITY

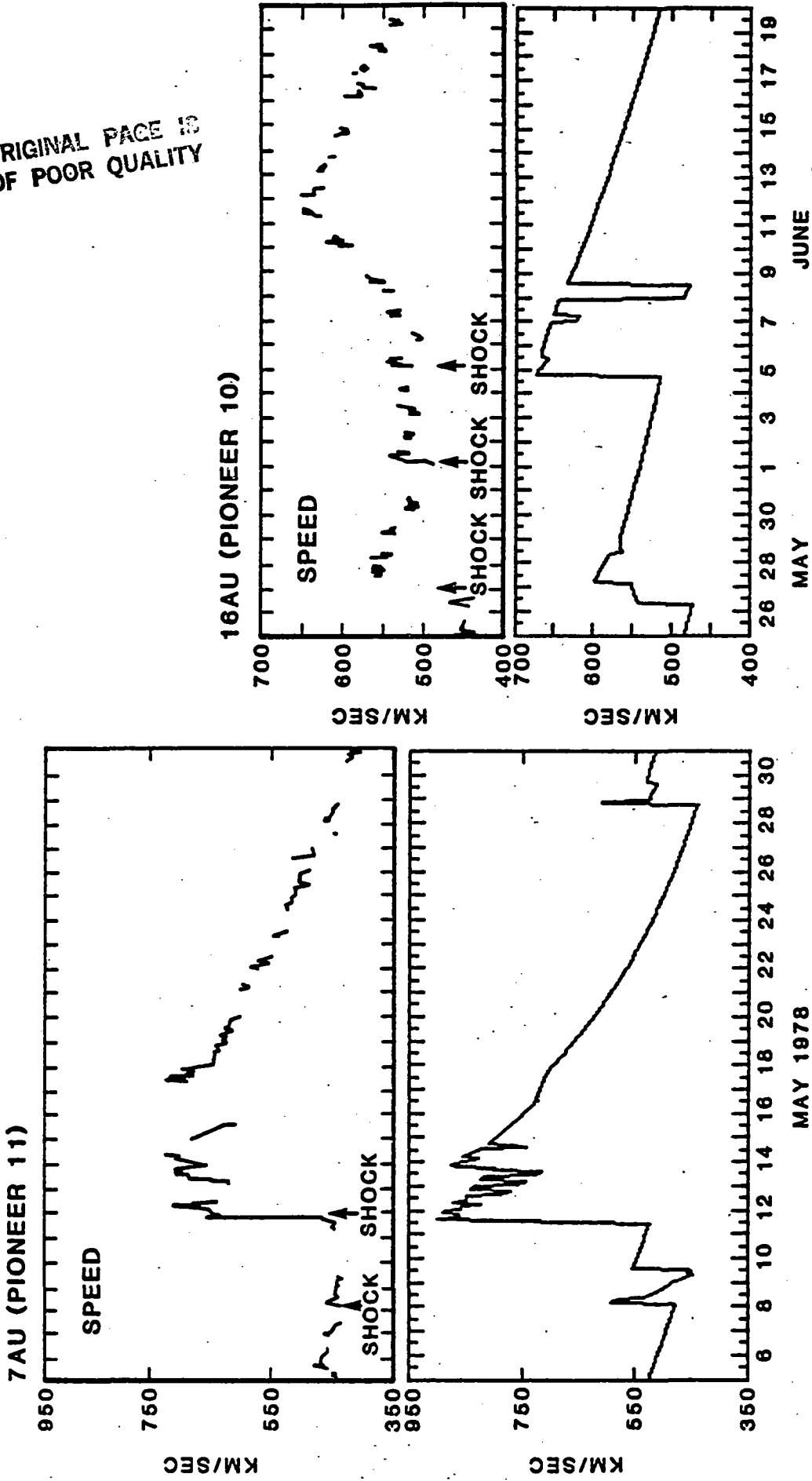


Fig. 15